PALAEO-ENVIRONMENT, DIAGENESIS AND CHARACTERISTICS OF PERMIAN BLACK SHALES IN THE LOWER KAROO SUPERGROUP FLANKING THE CAPE FOLD BELT NEAR JANSENVILLE, EASTERN CAPE, SOUTH AFRICA: IMPLICATIONS FOR THE SHALE GAS POTENTIAL OF THE KAROO BASIN

C. GEEL
AEON-ESSRI and Department of Geosciences, Nelson Mandela Metropolitan University, P.O. Box 77000, Port Elizabeth, 6031.
e-mail: geel.claire@gmail.com

M. DE WIT
AEON-ESSRI (Earth Stewardship Science Research Institute), Nelson Mandela Metropolitan University, P.O. Box 77000, Port Elizabeth, 6031.
e-mail: maarten.dewit@nmmu.ac.za

P. BOOTH
Department of Geosciences, Nelson Mandela Metropolitan University, P.O. Box 77000, Port Elizabeth, 6031.
e-mail: peter.booth@nmmu.ac.za

H-M. SCHULZ
Helmholtz Centre Potsdam- GFZ German Research Centre for Geoscience, Telegrafenberg, D-14473 Potsdam, Germany
e-mail: schulzhm@gfz-potsdam.de

B. HORSFIELD
Helmholtz Centre Potsdam- GFZ German Research Centre for Geoscience, Telegrafenberg, D-14473 Potsdam, Germany
e-mail: brian.horsfield@gfz-potsdam.de

ABSTRACT

We report on geochemical and petrophysical properties of shales from the Prince Albert, Whitehill and Collingham Formations of the Lower Karoo Supergroup, near Jansenville in the Eastern Cape, close to the tectonic front of the Cape Fold Belt. Results are based on two boreholes sited on a southerly dipping limb of a shallowly plunging syncline. Structural, sedimentological, lithological, mineralogical, geochemical and petrophysical analyses provide detailed characteristics that have become the focus of interest for potential shale gas occurrences.

The black shales of the Whitehill Formation are composed of quartz, illite, muscovite and chlorite, with lesser plagioclase and accessary pyrite. The Collingham Formation rocks have the largest proportion of quartz, which gives this formation a higher brittleness factor than that of the Prince Albert and Whitehill formations. Mercury porosimetry analyses yield average meso- and macroporosity values of 0.83% for black shales of the Whitehill Formation, confirming that these sediments are tightly packed. Layers of dolomite within the shales have porosities of 2.9%, and pores measuring 1.5 m wide.

The black shales of the Whitehill Formation have an average total organic carbon (TOC) content of 4.5 weight % whereas the TOC content of shales in the Collingham and Prince Albert Formations is <1 weight %. The elemental composition and relatively higher $\delta^{13}C$ and $\delta^{15}N$ stable isotope values suggest that the Whitehill Formation was deposited under anoxic conditions, which led to the preservation of the mixed marine and terrestrial organic matter, whereas the Prince Albert and the Collingham Formations were deposited under oxidizing conditions.

High maximum temperature values (Tmax average: 528^{o}C), low overall hydrogen and oxygen index values (all from Rock Eval analyses) and high reflectance measurements on bitumen (BR_o= 4%) characterise these sedimentary rocks as over mature. As a consequence, they display few hydrocarbon yields in pyrolysis and thermovaporization experiments, and offer a minor late-gas potential.

The main characteristics of black shales in the study area indicate that their overmaturity with respect to hosting gas deposits is attributed to the tectono-metamorphic overprinting during the Cape Orogeny (ca. 250 Ma, Hälbich, 1993; Hansma et al., 2015).

Rocks of the lower Karoo Supergroup outcropping within the area flanking the northern tectonic margin of the Cape Fold Belt therefore have limited potential for hosting shale gas deposits. This finding has implications for estimates of potential shale gas resources of the Karoo Basin.

Introduction

Shale gas is an unconventional resource originating in organic-rich black shales. It has become a major resource play in North and South America, China, and European countries since recent advances in horizontal well-drilling techniques, reservoir stimulation and induced fracturing of rocks (fracking) have provided advanced mechanisms to release gas held in "tight" shales (e.g. Ratner and Tiemann, 2013; Cook et al., 2013; CCA, 2014; Zoback and Arent, 2014). Discoveries of gas in the main Karoo Basin in South Africa appear to be an attractive option to meet the energy needs of the country and alleviate the pressure of coping with rising electricity costs. South Africa is 93% dependent on coal as an energy resource and with carbon taxes being implemented from 2015 (Macmullan, 2013), cleaner burning gas could reduce CO_2 emissions, provided gas leakage can be curtailed (e.g. Brandt et al., 2014), and risks associated with potential damage to environment and fresh ground water resources can be managed successfully (e.g. Stern et al., 2014; Small et al., 2014; Mauter et al., 2014). In addition, gas discoveries are punted to bring about related industries, thus potentially boosting economic growth through the provision of work and opportunities for local communities.

The Karoo Basin is an attractive target area for exploration of shale gas because of its extensive size, appropriate host rocks and potentially large resources of gas. Early estimates, based on a prospective area of between 155 000 and 183 000 km^2, were calculated to contain ca. 500 trillion cubic feet (Tcf) potential reserves as risked recoverable gas in place (e.g., Kuuskraa et al., 2011). Subsequent studies suggested that these numbers are over-optimistic and may rather fall within a probabilistic range of ca. 14-172 Tcf (with a median of ca. 50 Tfc; Decker and Marot, 2012; J. Decker, personal communications, 2014; and PASA unpublished data). Considering that Mossgas was built on ca. one Tcf highlights the potential of the Karoo reservoirs nonetheless.

However, two factors that influence the potential gas content and the distribution of gas are: (i) proximity, to the south, of the host rocks to the Cape Fold Belt (CFB), and (ii) proximity, to the north, of the host rocks to multiple dolerite intrusions, especially north of the southern Africa escarpment.

In the first example deformation and metamorphism of all strata occurring within the tectonic front of the CFB may have expelled all (or most) of the gas during the Cape Orogeny focused at about 250 Ma (with a possible range of 276 and 248 Ma; Hälbich, 1993; Hansma et al., 2015). In the second case, contact metamorphism of gas-bearing strata adjacent to the 183 to 182 Ma dolerite intrusions (Svenson 2012; Burgess et al., 2015), related to the ca. 183 Ma Karoo large Igneous Province (e.g. Duncan at al., 1997), may have induced significant gas loss due to thermal devolatisation (Svensen et al., 2006; 2007; 2008). For example, based on detailed core analyses, Aarnes at al. (2010; 2011) calculate that devolatilization during sill intrusions may have caused 2700 to 16200 gigatons of gas loss across the Karoo Basin (South Africa). However, the effects of thermal devolitisation are still difficult to quantify with reasonable certainty, since the metamorphic aureole thicknesses can vary from 30% to 200% of the sill thickness, depending on host-rock temperature, sill thickness and intrusion temperature. Indeed Maré et al., (2014), used magnetic techniques on one borehole to determine palaeo-temperatures in Ecca Group shales intruded by dolerite sills and found that the greatest thermal effects are limited to thin contact aureoles, suggesting that significant volumes of shale outside the contact aureole may potentially still contain gas.

Considering the above factors, companies have taken out concessions to explore for shale gas in the most favourable region between the frontal ranges of the CFB to the southern Karoo escarpment and northwards thereof. With the South African Government's cabinet approval, exploration has commenced with a first phase of desk-top studies, to be followed by geophysical surveys and exploratory core drilling over the next 2 to 5 years (Twine and Jackson, 2012; Ensor, 2013).

The aim of this contribution is to address the geoscientific suitability of black shales flanking the CFB as a potential unconventional gas reservoir. The study set out to provide subsurface geological, geophysical and geochemical data of the lower Ecca Group (Southern Karoo Basin) in an area between Jansenville and Wolwefontein in the Eastern Cape Province (Figure 1). This area was chosen because of rock outcrops from the lower Ecca Group that are also affected by the deformation of the CFB and are representative of the general area within its tectonic front.

Two shallow boreholes were sited to retrieve fresh core from the Ecca Group. Core samples were then analysed for their mineralogical, geochemical and petrophysical properties.

Regional geology of the Karoo Basin

Karoo Basin

The Karoo Basin formed as a successor basin to the early Palaeozoic Cape Basin along the south-western margin of Gondwana. The origin of the Karoo Basin is controversial. It has been interpreted as a retro-arc foreland trough formed by shallow-angle, north-dipping subduction of the palaeo-Pacific plate beneath Gondwana supercontinent that led to the building of the

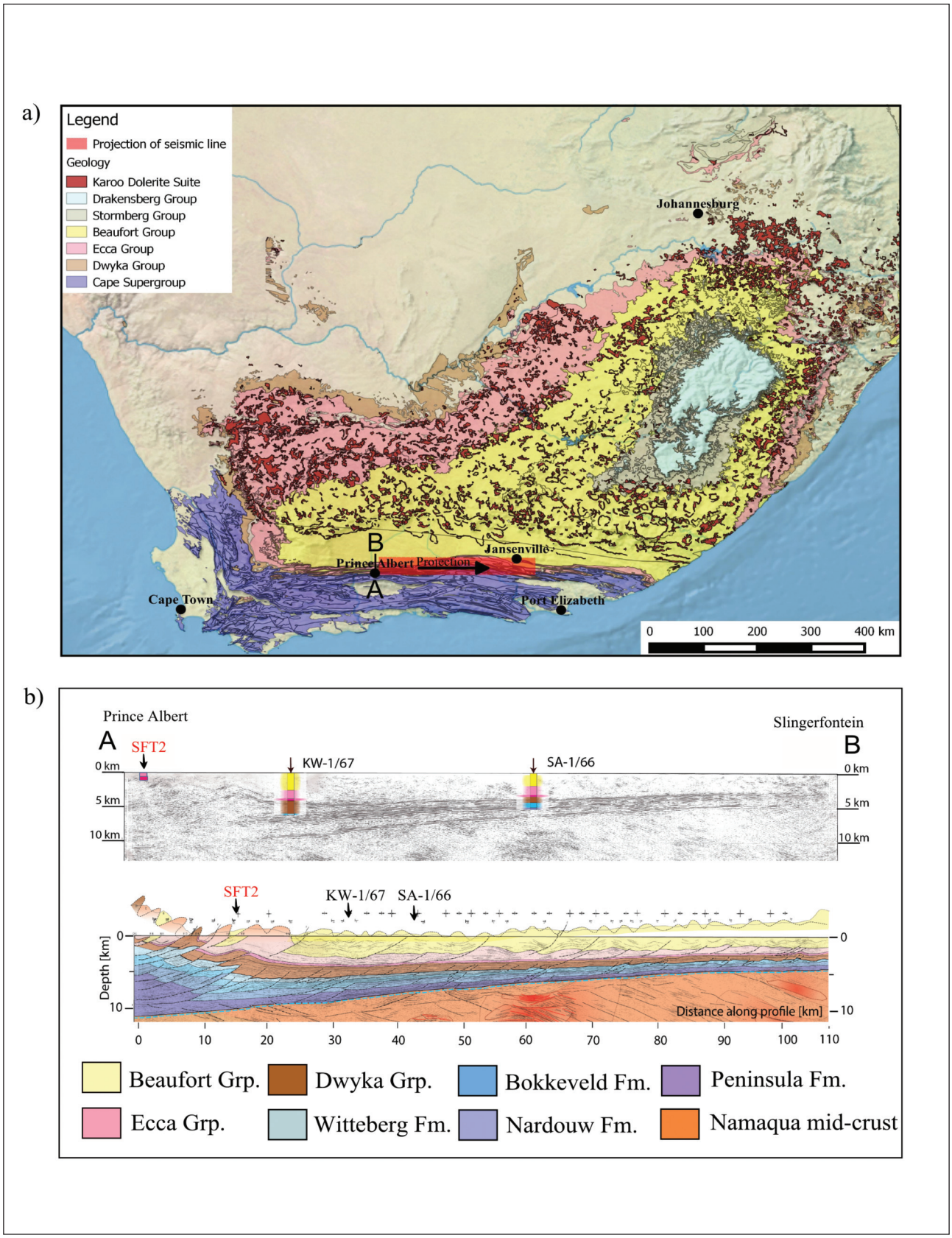

Figure 1. *(**a**) Regional geology of the Karoo Basin showing locality of study area and collective concession prospecting area. Note location of seismic line surveyed by Lindeque et al.,(2011), relative to study area (SFT2). The exact location of the seismic line is from Prince Albert to Slingerfontein in the Western Cape. (**b**) Seismic profiles and position of boreholes (KW-1/67 and SA-1/66) drilled by SOEKOR during oil exploration in the 1960's. Note that borehole SFT2 in the study area, is shown projected on to the seismic section. Interpretation of seismic data by Lindeque et al.,(2011) shows numerous south-dipping thrust faults disrupting the strata of the Cape and Karoo Supergroups.*

Figure 2. *Dolomite concretions documented near Mount Stuart and Jansenville, in the Eastern Cape.*

Cape Fold thrust belt (e.g. Lock, 1980; Catuneanu et al., 2005; Johnson et al., 2006). In this model a volcanically active source area is believed to be situated somewhere north of the palaeo-Pacific subduction zone, modeled as a foredeep, forebulge and back-bulge flexural province (Catuneanu et al., 2005).

Tankard et al. (2012) contested this model by pointing out that there is no evidence for a nearby magmatic arc and that the Karoo Basin fill does not show evidence of on-lapping characteristics of a flexural foreland basin. These authors proposed that the detailed Karoo stratigraphy is linked to the behaviour of rigid crustal blocks and their weak boundary fault zones comprising the southern African lithosphere. Taking these factors into consideration these authors interpreted the Karoo Basin as a sinistral strike-slip orogen linked to oblique reactivation of a southern Namaqua suture. Boundary forces associated with the CFB created the late Karoo foreland basin (De Wit and Ransome, 1992; Tankard et al., 2012).

In an attempt to elucidate the nature and configuration of the basement rocks below the Karoo strata, Lindeque et al., (2007; 2011) carried out a long, high resolution, near-vertical seismic reflection profile through the Cape-Karoo Basin and the underlying basement rocks (from Prince Albert to Slingerfontein in the Western Karoo basin). The data from this seismic survey (Figure 1) show the Karoo Basin to be ca. 5 km deep at the frontal margin of the CFB, consistent with earlier interpretations from well data (Rowsell and De Swardt, 1976; Scheiber-Enslin et al., 2014a). This is in sharp contrast to the 12 km as is generally accepted to be the basin's thickness at the southernmost margin of the Karoo Basin (e.g. Cole, 1992; Cloetingh et al., 1992; Johnson et al., 2006). However, the latter estimates are all based on estimated strata thickness in the southeastern part of the basin (e.g. Cole 1992; Johnson et al., 2006). This is also the region where significant repetition of strata has been documented across numerous exposed, but mostly concealed thrusts, despite the generally poor outcrop here (Booth and Shone, 1999; 2002; Paton et al., 2006; Newton et al., 2006; Booth and Goedhart, 2014), which have not yet been included into a revision of the lithostratigrapahy, a need advocated by Booth and Shone (1999, 2002) for both the Cape and Karoo Supergroups in these areas.

There is therefore no robust evidence for substantial thickening of foredeep sequences as modelled for a retroarc foreland basin (e.g. Lock, 1980; Hälbich, 1993; Johnson et al., 2006). The suggested northward subduction model does not fit the deep seismic reflection data, as there does not appear to be a deep suture zone directly beneath the CFB and/or the Cape-Karoo Basin sequences (Lindeque et al., 2011; Scheiber-Enslin et al., 2014b). The Karoo Basin also does not bear the lithostratigraphic similarities to a typical foreland basin. It is therefore suggested that the frontal range of the CFB and the Karoo Basin may represent a thin-skinned Jura-type fold belt formed as a consequence of collision and suturing south of the CFB, related to south-dipping subduction to the south (Paton et al., 2006; Lindeque et al., 2011).

Deposition of Karoo sedimentary rocks

The Karoo Basin archives about 170-160 million years of sediment accumulation (from ca. 350 to 340 Ma to ca. 180 Ma) during the heydays of Gondwana (Isabell et al., 2008; Milani and de Wit, 2008; Linol et al., 2015; McKay et al., 2015). The Karoo Supergroup is stratigraphically divided into several groups defined by their age and contrasting sedimentological characteristics: Dwyka, Ecca, Beaufort, Stormberg and the Drakensburg Groups (Johnson et al., 2006).

After the deposition of the Cape Supergroup in the Cape Basin, there was a period of uplift and erosion. Ice sheets waxed and waned along the southern margin of the Gondwana continent marking the period of Dwyka glaciation that lasted between ca. 350 Ma and ca. 290 Ma (Bangert et al., 1999; Isabell et al., 2008; Milani and de Wit, 2008; Tankard et al., 2012). During glaciation an extensive shallow lake formed, fed by meltwater during glacial retreats (interglacials), resulting in the deposition of the Dwyka diamictites (Smith, 1990). Some authors have inferred that the Dwyka diamictites and lower Karoo were deposited in an open marine setting (eg. Smith, 1990; Visser, 1992). Others have proposed a lacustrine environment that persisted during the deposition in the Whitehill Formation (Faure and Cole, 1999). This inter-continental lake was subsequently terminated by a short marine transgression related to eustatic sea level rise as a response to final deglaciation (e.g. Milani and de Wit, 2008).

The first post-glacial sequence is the Prince Albert Formation, which is dated at 289 to 288 Ma by U-Pb on zircons from air-fall tuffs close to the boundary of the Dwyka Group (Bangert et al., 1999; Tankard et al., 2012; McKay et al., 2015). The Prince Albert Formation contains dropstones near the base and consists mostly of

mudstone, shales and some thin sandstone units (Geel et al., 2013; Cole, 2005).

Homogenous black mudstones of the Whitehill Formation overly the Prince Albert Formation and comprise fine-grained, finely laminated black organic-rich shales that weather white at surface due to pyrite oxidation to gypsum (Geel, 2014; Wickens, 1994; Visser, 1992). Dolomite lenses and concretions are present between layers of black shale (Figure 2). Contrary to the massive Dwyka sequences, shale beds of the Whitehill Formation are disharmonically folded and commonly interpreted as a regional 'décollement' surface (Kingsley, 1977; Lindeque et al., 2011).

The Whitehill Formation is overlain by thin bedded turbidites, dark grey mudstones and tuff beds (K-bentonite) of the Collingham Formation. Zircons from the tuffs have been dated between ca. 276 and 270 Ma (e.g. Fildani et al., 2009; McKay et al., 2015). The mudstones contain trace fossils such as *Planolites* and other epichnial grooves. At the top of the formation the mudstone grades into sandstone that contains plant impressions (*Glossopteris* sp.) (Viljoen, 1994). Pyrite is common in the lower half of this formation.

These sequences are overlain by turbiditic sandstones and minor mudstones of the Vischkuil, Laingsburg and Ripon formations followed by basin plain and prodelta mudstones and rhythmites of the Fort Brown Formation and then increasingly by deltaic sandstone and minor mudstone of the Waterford Formation, culminating in terrestrial mudstone, siltstone and sandstone of the Beaufort Group (Kingsley, 1981; Smith et al., 1993; Rubidge et al., 2000; 2012; van der Merwe et al., 2010). Tuffs in the Koonap, Middleton and Balfour Formations of the Beaufort Group in the south-eastern part of the basin have been dated at between 261 and 255 Ma (U-Pb zircon; Rubidge et al., 2013) and in the Abrahamskraal Formation of the Beaufort Group in the south-western part of the basin at between 276.4 and 260.6 Ma (U-Pb zircon; Lanci et al., 2013; McKay et al., 2015). Thereafter, following northward migration of the deformation front of the CFB (e.g. Booth and Goedhart, 2014), there was uplift of the basin with increasingly arid climate conditions (Smith and Botha-Brink, 2014), terminating with aeolian deposition of the upper Stormberg Group. The final stages of Karoo deposition constitute widespread sand-dune sequences of the Clarens Formation, which was interrupted by the volcanism of the Drakensberg Group that brought the Karoo depositional sequence in South Africa to an end at ca. 183 Ma (Duncan et al., 1997). In the early Jurassic (183 to 182 Ma) dolerite sills and dykes of the Karoo Large Igneous Province intruded into mainly the Ecca and Beaufort Groups (Svensen et al., 2006; Aarnes et al., 2011; Burgess et al., 2015). Following extensive upper Cretaceous erosion and exhumation of southern Africa, these massive igneous intrusions formed a regional escarpment flanking the southern Karoo (Duncan et al., 1997; Tinker et al., 2008; Decker et al., 2013).

The Cape Fold Belt

Prior to Gondwana break-up, the CFB formed part of the greater Gondwanide orogenic belt that extended west into South America and east through the Falkland Islands and Antarctica as far as the eastern margin of Australia (Veevers, 2004; Linol et al., 2015). The structural style of the CFB includes both thin-skinned and thick-skinned deformation and consists of anticlinoria featuring overfolds, thrusts, *en enchelon* folds and faults, flower structures and low angle and strike-slip step over structures. Metamorphism of the CFB grades to greenschist facies in the south and overprints proximal Karoo lithologies in the north (Hälbich, 1993; Tankard et al., 2012; Booth and Goedhart, 2014).

Field observations and location of drill sites

The study area (Figure 3, topocadastral sheet 3324BB; Greystone; scale 1:50 000) was chosen after taking into account the amount of outcrops of the lower Ecca Group rocks and road access to the field area and potential drill sites. Field mapping was carried out with the use of air photos, from which geological and structural data were transferred onto the topocadastral sheet. Structural data obtained from the field determined fold plunges and aided in siting two shallow boreholes (SFT1= 100 m deep and SFT2= 300 m deep). Core was sampled from drill hole SFT2 for detailed analyses. Core from both boreholes is stored at AEON, Nelson Mandela Metropolitan University (NMMU).

A total of 52 samples of core from the Prince Albert, Whitehill and Collingham Formations were collected for TOC/Rock Eval Pyrolysis. 16 samples from the 52 were selected for the following analyses: X-ray fluorescence (XRF), X-ray diffraction (XRD), Hg-intrusion porosimetry, open pyrolysis and thermovaporation, vitrinite reflectance, and C/N stable isotope analyses.

All analyses were completed at the Helmholtz Centre, GFZ, Potsdam in Germany, over a period of 11 months, except for vitrinite reflectance measurements, which were undertaken at Aachen University, Germany.

Results

Structural geology

A north-south cross section through the Greystone area indicates that there are four mega- folds in the region, annotated 1 to 4 in Figure 3. The folds are all open except for the anticline at locality 2. Smaller parasitic folds are seen throughout the area and in general the folds plunge towards the southwest. Field observations of the Whitehill Formation show that the shales are highly folded when compared to the underlying Prince Albert Formation and the overlying Collingham Formation. A large fault strikes east to west along the limb of the overturned anticline. Normal and reverse faults occur throughout the area and are seen with increasing frequency closer to the CFB front in the south. Rose diagrams plotted for subareas of the Greystone 1:50 000 sheet show that main joint directions are prominently north-northeast to south-southwest and westeast.

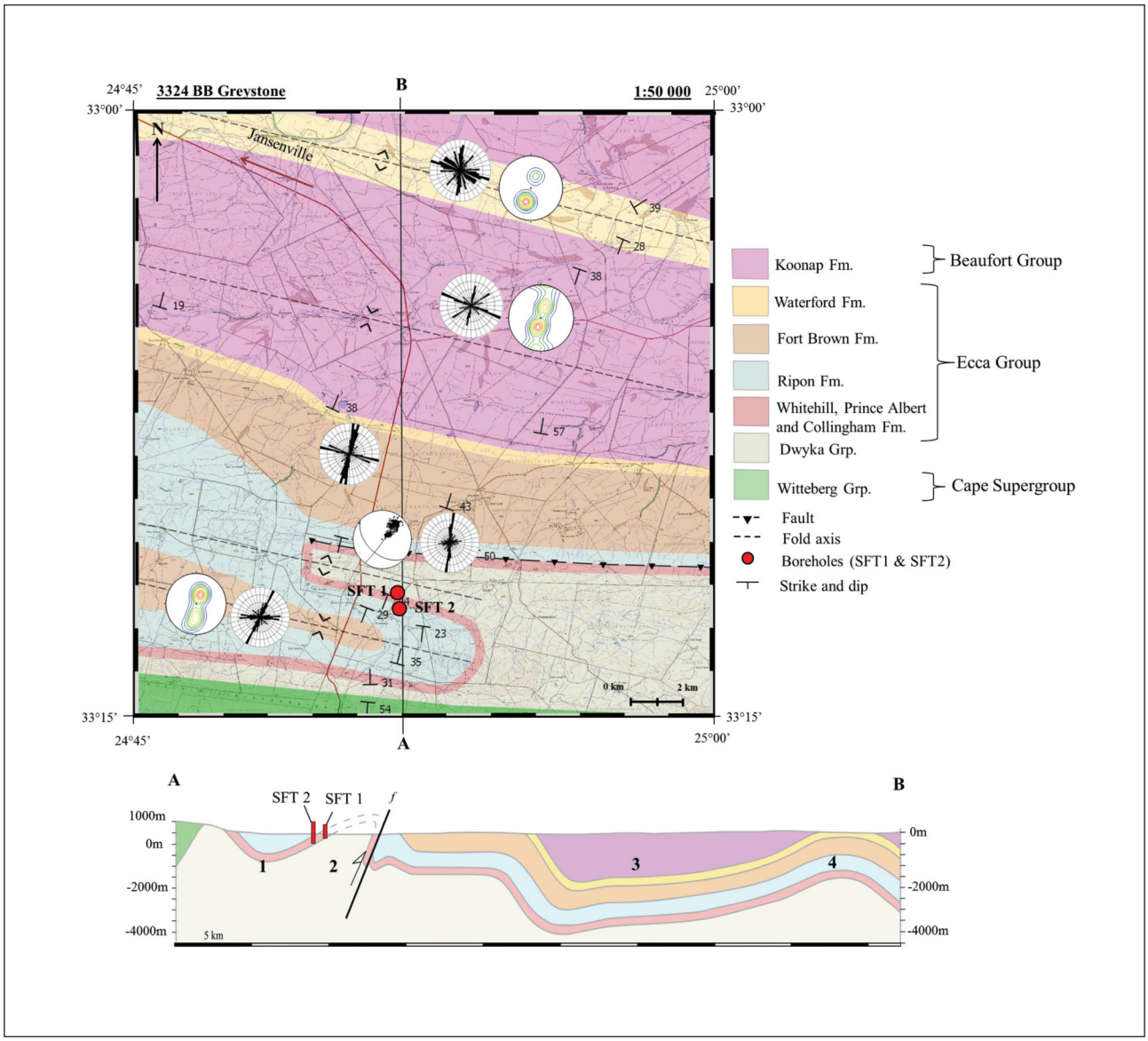

Figure 3. *Geological map and cross section (**A-B**) through the Greystone area. Four mega-folds (labelled 1 to 4) are indicated on the cross section, as well as the location of boreholes SFT 1 and 2. Stereograms on the map are of bedding, plotted as poles to planes, on equal area nets. Note that the folds are mostly open and north vergent, with shallow plunges, with exception of anticline 2. Joint orientations are shown as rose diagrams which show two dominant strike orientations, viz. northsouth and west-northwest.*

A simplified litho-stratigraphic column (Figure 4) of borehole SFT 2 was drawn using field data and core logs, also indicating the horizons where the 16 samples were taken.

Lithology

Witteberg and Dwyka Groups

Pale grey coloured quartzites and khaki colored shales of the Late Palaeozoic Witteberg Group form a prominent ridge in the southern part of the area, whereas the overlying Dwyka, Ecca and Beaufort Groups of the Karoo Supergroup occur in the remainder of the study area (Figure 3). The Dwyka Group crops out in the anticlinal hinges of the open folds in the southern half of the area, and is composed of grey compact diamictites containing clasts of variable size and composition in a very-fine grained, grey coloured clay matrix.

Ecca Group

Drillhole data show that the Prince Albert Formation in this area is 59 m thick and has a gradational contact with the underlying Dwyka Group. This Prince Albert Formation consists mostly of an olive-grey mudrock. Siltstones and shales are rhythmically interbedded with the mudstones (Figure 5g). They are mostly horizontally laminated, composed of tightly packed clay layers (Figure 5h) that occasionally display water escape and flame structures. Phosphate and carbonate lenses were identified in the field and oxidized iron-rich bands are found between mudstone layers. Tuff layers occur in the lower half of the formation. Foraminifera (possibly a

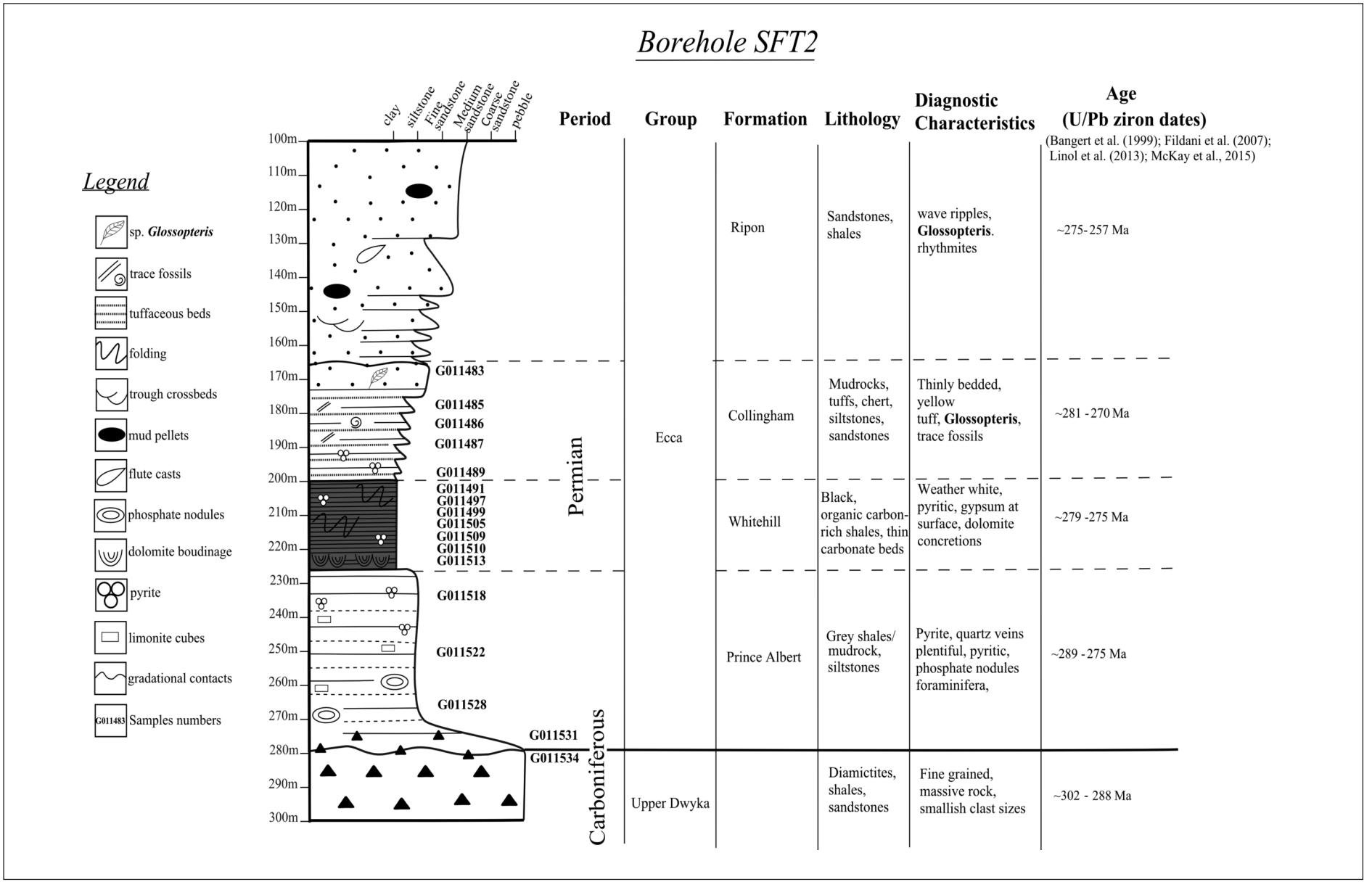

Figure 4. *Litho-stratigraphic log of borehole SFT 2 showing position of samples. Note that U/Pb zircon dating of tuff horizons bracket the lower three formations of the Ecca Group between 289-270 Ma.*

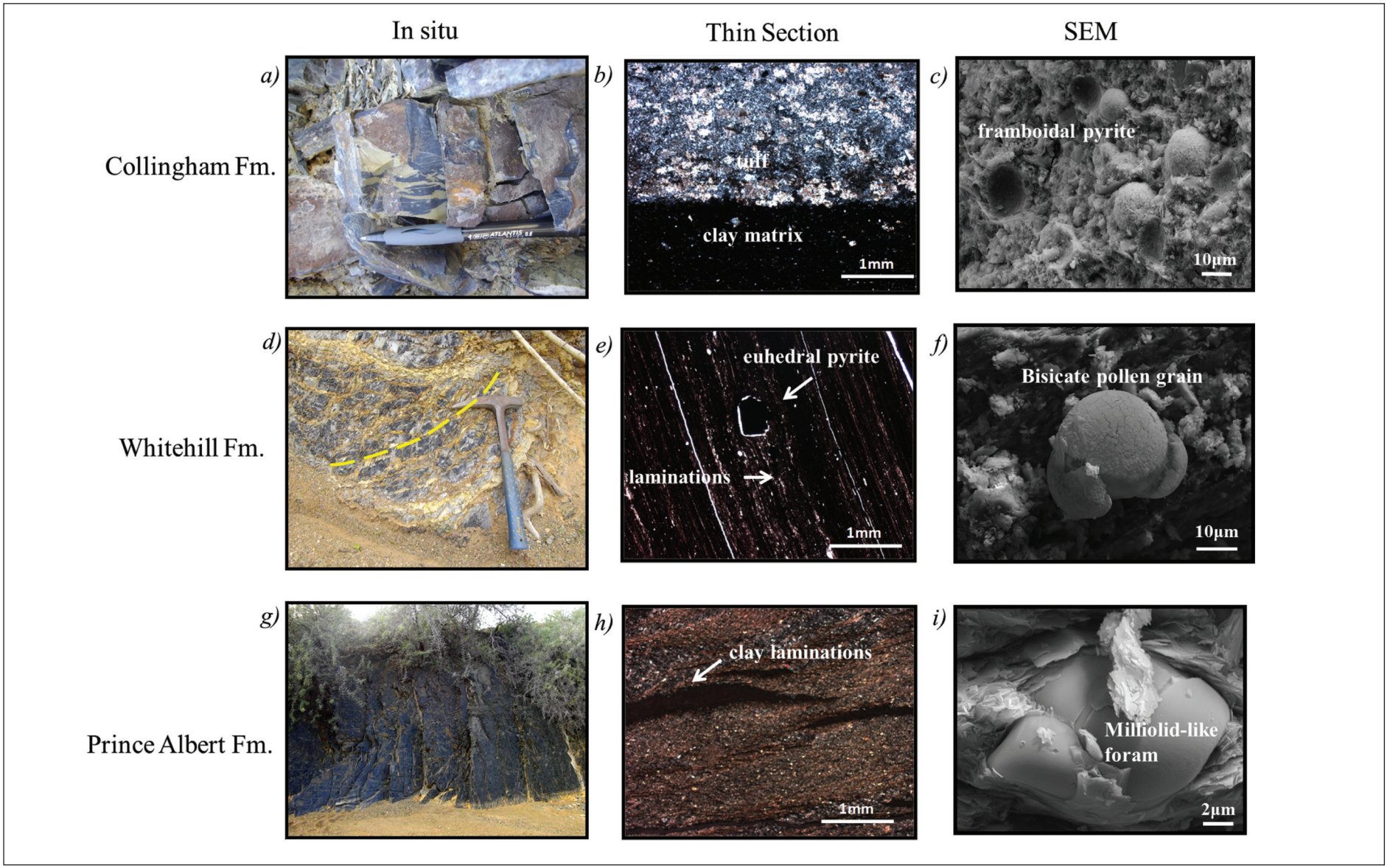

Figure 5. *Photographs (first column) showing typical outcrops of the Prince Albert, Whitehill and Collingham Formations in the study area. The second column shows common features of the rocks in thin sections of these formations. The last column shows SEM micrographs of fresh core from borehole SFT 2, where micro-fossils and nature of pyrite grains are clearly visible.*

juvenile miliolid) were observed under scanning electron microscope (SEM) and thin section analysis showed recrystallization and alteration features.

The Whitehill Formation is some 27 m thick (drillhole data), and forms a gradational contact with the underlying Prince Albert Formation. The Whitehill Formation consists mostly of black shale (Figure 5d). The black shales are occasionally interlayered with grey, fine-grained siltstone layers. Dolomite concretions occur near the base of the formation. The dolomite contains internal concentric laminations which sometimes follow the external form or are intensely convoluted. At surface the shales weather white due to an oxidation reaction between pyrite (FeS_2) and dolomite ($CaMg(CO_3)_2$) to form gypsum ($CaSO_4 \cdot 2H_2O$) growing in veins, crystal masses or desert roses. Pyrite within the shales also creates oxidation staining and the weathered shales vary in surface colouration (white, grey or pink). The Whitehill shale comprises mostly clay minerals (e.g. illite, muscovite and quartz). A bisicate pollen grain was detected by SEM micrograph (Figure 5f). Thin section analysis reveals framboidal and euhedral pyrite (Figure 5e) and remnants of trace fossils (possibly miliolid). SEM micrographs of the dolomite show a greater degree of porosity than other rock types in this formation.

The Collingham Formation, a grey mudstone, is distinctly jointed, well layered and intercalated with tuff in the field (Figure 5a). The mudstone facies varies within the formation, in some cases exhibiting pencil fracturing. The Collingham Formation is ca. 35 m thick, and has a sharp contact with the underlying Whitehill Formation, grading upwards into fine-grained sandstone at the top of the formation, which contains imprints of leafy plant material (*Glossopteris?*). Trace fossils, most commonly *Planolites* and *Scolicia*, are seen on the bedding surfaces of the mudstones. At the top of the formation mudstone grades into sandstone that contains plant and wood impressions (*Glossopteris?*). Under the light microscope, the boundaries between clay minerals and the tuffs can be observed (Figure 5b), and SEM analysis revealed that framboidal pyrite occurs close to the contact with the Whitehill Formation (Figure 5c).

In the eastern Karoo Basin the Vischkuil and Laingsburg formations do not occur (Johnson et al., 2006). The Ripon Formation overlies the Collingham Formation and is characterised by alternating layers of mostly grey coloured sandstones, greywackes, mudstones, siltstones and shales. The sandstones exhibit wavy bedding, trough cross stratification, convolute laminations and hummocky cross stratification, whereas shales exhibit slump and dewatering structures common in turbidites. Trace fossils (*Scolicia?*) and plant impressions are common on mud and sandstone surfaces.

The Fort Brown Formation is composed of alternating sandstones, siltstones and mudrocks (rhythmites). Most beds are delaminated but occasional trough cross-beds occur, as well as ripples, convoluted bedding and occasional dewatering structures.

The Waterford Formation comprises sandstone of variable colour, mudstone, siltstone and shale beds. The sandstone particularly displays well developed ball and pillow structures. Gastropod tracks, fish trails and other trace fossils are common on rippled bed surfaces.

Beaufort Group

The lower Koonap Formation outcrops in the northern portion of the study area and comprises lenticular yellow-brown sandstones, grey sandstones, grey mudrocks and maroon and grey-green siltstones. Sandstone units make up less than one third of the sequence and display laminated and cross-bedded features typical of fluvial sediments.

Mineralogy

X-ray diffraction

X-ray diffraction (XRD) analyses showed the following results averaged for minerals in the main rock types of the lower Ecca Group:

- Prince Albert Formation: quartz (52%), illite (21%), muscovite (23%), chlorite (4%) and pyrite (0.2%). Sample G011534 from the gradational contact between the Dwyka Group and the Prince Albert Formation has a mineralogical composition of: quartz (53%), illite (21%), anorthite (8%), muscovite (15%), chlorite (3%) and pyrite (0.2%).
- Whitehill Formation: quartz (32%), calcite (6%), albite (7%), illite (16%), muscovite (15%), chlorite (8%), pyrite (7%) and dolomite (9%). The mineralogical composition of sample G011513 comprises mostly dolomite. The weathering of pyrite, dolomite and calcite contents caused the formation of gypsum.
- Collingham Formation: quartz (62%), calcite (2%), albite (10%), muscovite (10%), chlorite (8%), biotite (3%), illite (13%) and pyrite (0.3%).

Shales with a higher percentage of quartz and carbonate tend to be more brittle, which responds to stimulation in a form of greater density of fractures along which gas can potentially flow into a well bore. If the shale is high in clay it will respond by ductile deformation, forming fewer fractures, limiting the ability to extract potential gas (Jarvie et al., 2007; Wang and Gale, 2009; Wang and Carr, 2012). The Whitehill Formation shales have high quartz content and the presence of dolomite within the shales also increases their brittleness factor.

Geochemistry

X-ray fluorescence

X-Ray fluorescence (XRF) data are normalised to aluminium and plotted as compositional ratios (Figure 6) SiO_2/Al_2O_3 ratios are the highest in the Prince Albert and the lowest in the Whitehill Formation. CaO and MgO peaks occur at the base of the Whitehill Formation, which corresponds with the occurrence of carbonate rock. The dolomite sample also shows peaks in barium and phosphorus, which suggests an increase in palaeo-productivity (Brumsack, 2006; Baioumy and Ismael, 2010).

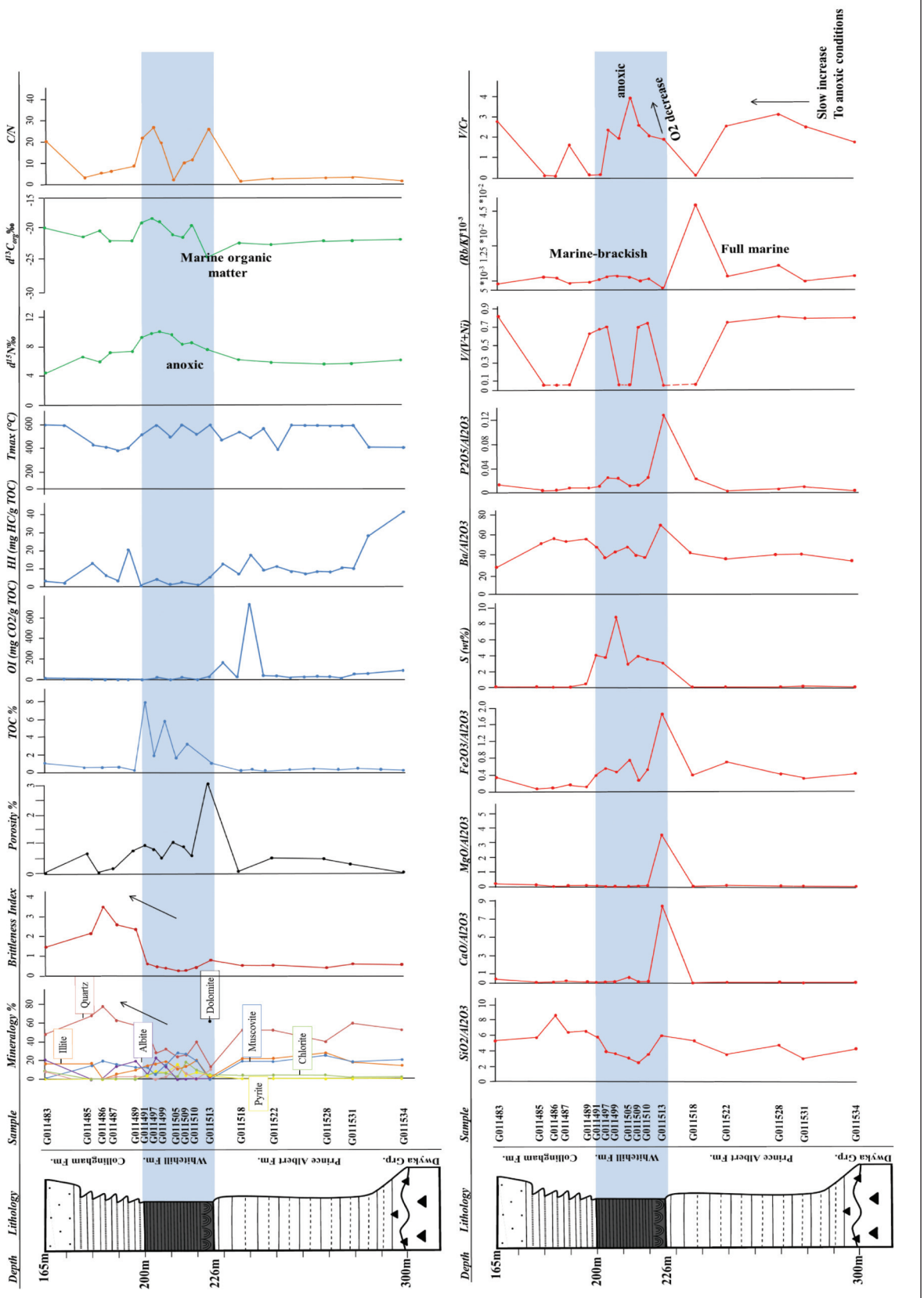

Figure 6. *XRF, XRD (vol. %), TOC (wt. %), $\delta^{15}N$ and $\delta^{13}C$ stable isotopes, and TOC/Rock Eval data plotted as depth profiles relating to the Prince Albert, Whitehill and Collingham Formations.*

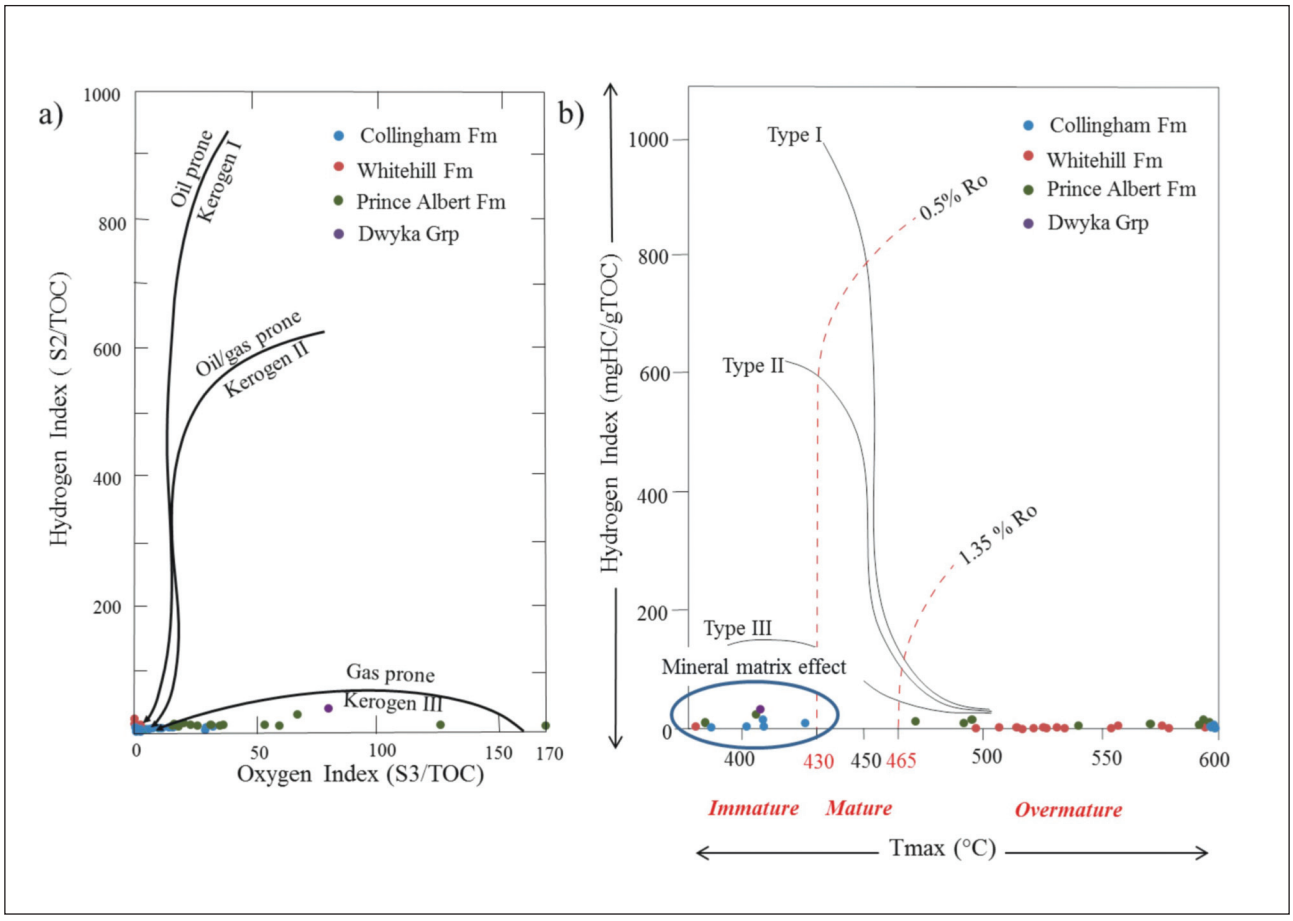

Figure 7. *Modified van Krevelen Diagrams showing (**a**) Hydrogen index (HI) vs Oxygen Index (OI); (**b**) Hydrogen index vs Tmax. Note that in (a) all samples of the Prince Albert Formation plot in the Kerogen III field and in (b) samples are predominantly overmature.*

Rb/K ratios may indicate changes in palaeo-salinity (Scheffler et al., 2006). In the Prince Albert and Whitehill formations there is a steady increase to higher Rb/K ratios, suggesting increasing marine conditions. V/Cr and V/(Vi+Ni) ratios are indicators of palaeo-redox conditions (Scheffler et al., 2006; Hatch and Leventhal, 1992; Rimmer, 2004). This data suggests that marine conditions and anoxic waters persisted during deposition of the Whitehill Formation until they become more brackish during the Collingham Formation.

Sulfur contents and Fe_2O_3/Al_2O_3 ratios peak in the Whitehill Formation (Figure 6). These data from the Whitehill Formation plot in the "anoxic zone" in an iron-sulfur-TOC (total organic carbon) ternary diagram. Data points along the stoichiometric pyrite line (S=1.15 Fe) suggest that all of the iron has been fixed as pyrite (Figure 8). Samples below the line suggest that sulfur occurs as oxide, e.g., barite, or bound to the organic fraction.

Organic geochemistry

TOC/Rock Eval

The average (TOC) content of shale in the Prince Albert Formation is 0.37 weight %, in the Whitehill Formation 4.5 weight %, and in the Collingham Formation 0.62 weight % (Figure 6). Rock Eval analyses produce S1 and S2 hydrocarbons. S1 represents hydrocarbons already produced and stored within the pores and S2 represents hydrocarbons produced from the thermal break-up of kerogen (Baceta and Nunez-Betelu, 1994). S1 and S2 values from Rock Eval analysis are low for all samples, reflecting low hydrocarbon yield or potential. Tmax values from Rock Eval analysis range between 460-572°C for the Prince Albert, Whitehill and Collingham Formations, categorizing these sedimentary rocks as late- to post-mature. A comparison for TOC contents, HI (hydrogen index), OI (oxygen index) and Tmax values is also shown in modified Van Krevelen diagrams (Figure 7). Note that relatively high OI values (suggesting derivation from terrestrial material) or low Tmax values (suggesting immature conditions) are caused by artificial mineral-matrix effect due to low TOC contents.

Stable isotope analysis ($\delta^{15}N$, $\delta^{13}C$)

The average $\delta^{13}C$ values for the rocks of the lower Ecca Group are:

- Prince Albert Formation:
  -23‰ (ranges: -22.6‰ to -23.8‰),
- Whitehill Formation:
  -20‰ (ranges: -18.9‰ to -24.7‰)
- Collingham Formation:
  -21.4‰ (ranges: -20.1‰ to -22.4‰).

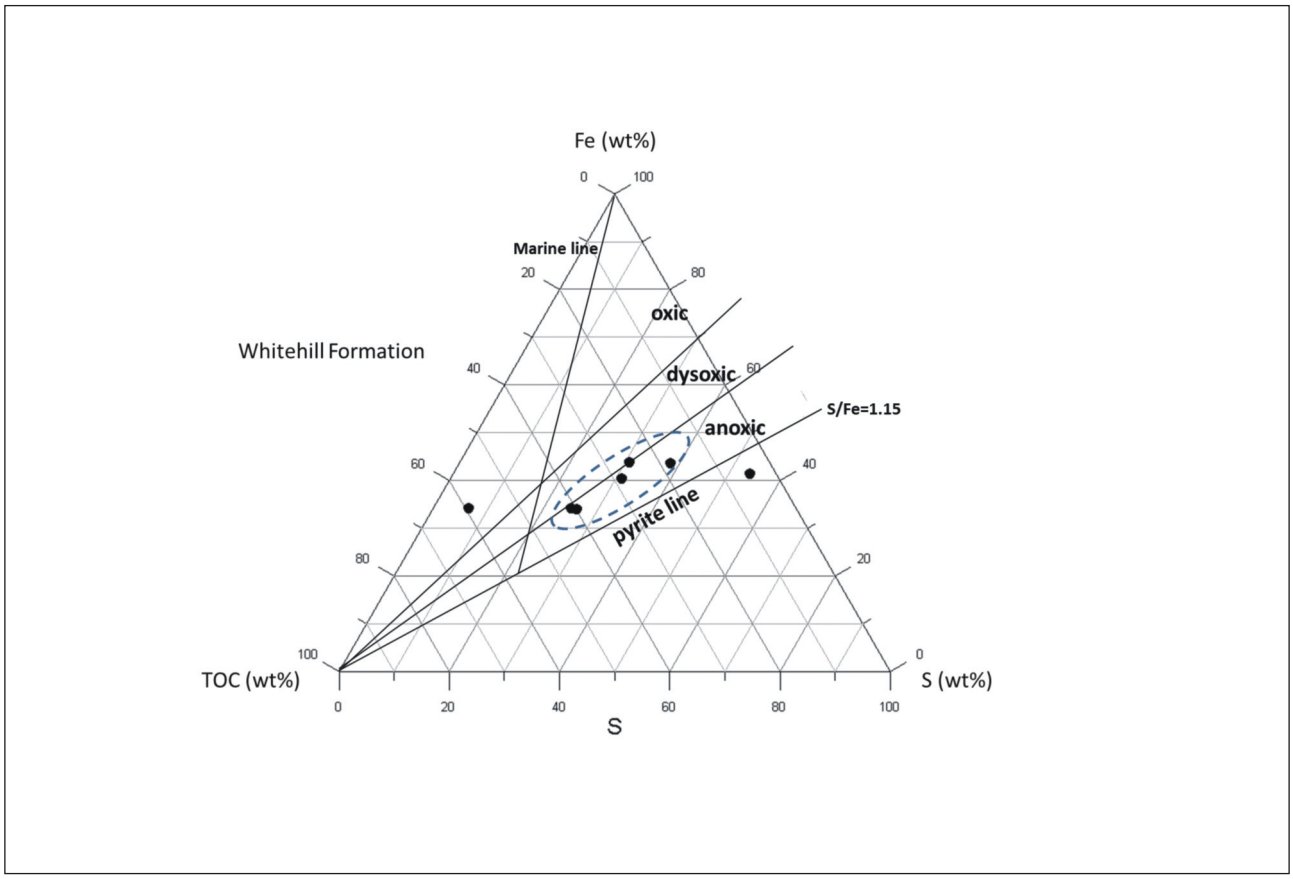

Figure 8. *Ternary diagram (Fe-TOC-S) showing oxidation conditions in the Whitehill Formation (interpretation based on original by Dean and Arthur, 1989).*

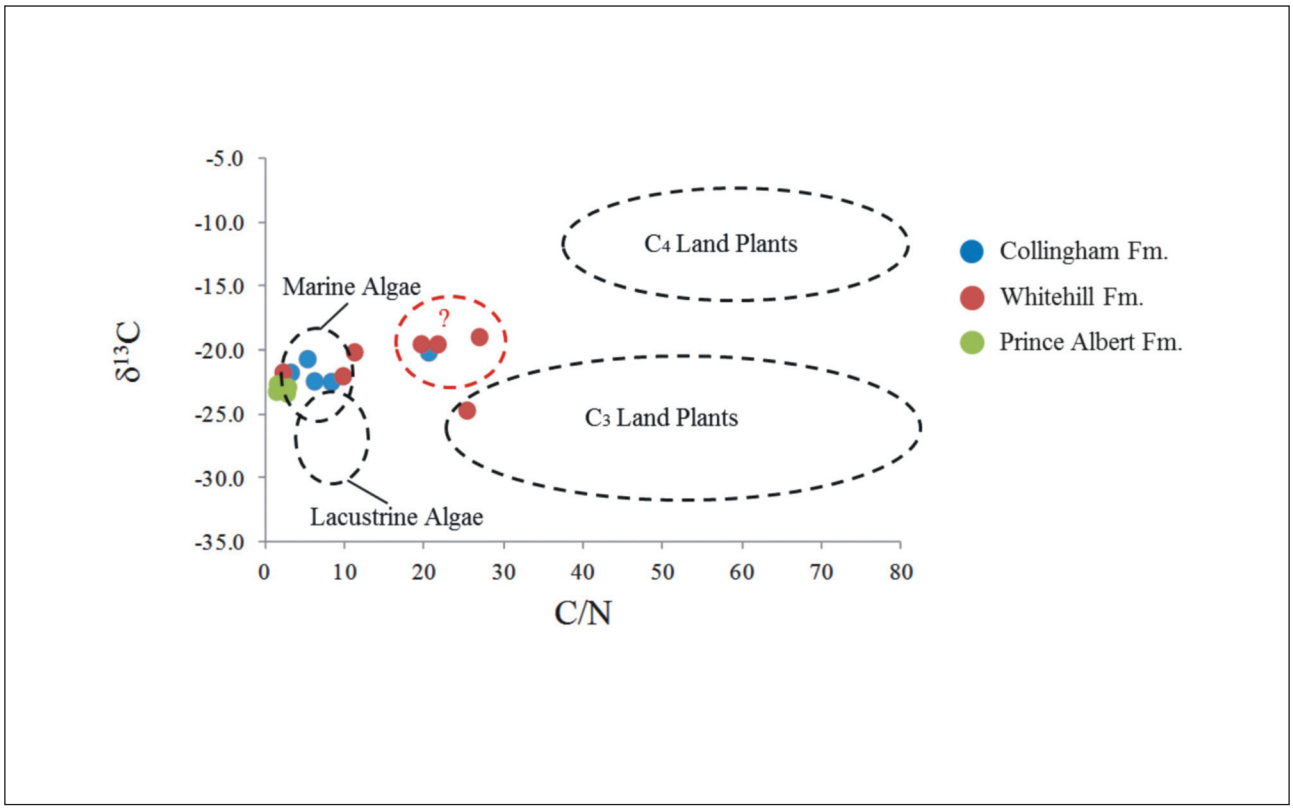

Figure 9*. C/N ratios and $\delta^{13}C$‰ values plotted within zones of different organic material sources.*

According to White (2013) and Meyer (1994) such values suggest an aquatic (mostly marine) organic source for all three formations. This is, however, not consistent with the C/N data. C/N ratios and $\delta^{13}C$ ‰ values, when plotted against each other, show that the samples of the Prince Albert Formation fall entirely in the marine algae zone, together with most of the Collingham and some of the Whitehill Formation samples. Three samples from the top of the Whitehill Formation and one sample from the top of the Collingham Formation do not fall in any definitive zone. One sample of the Whitehill Formation falls within the C_3 terrestrial plant zone. The Whitehill Formation values that do not fall in any particular zone all have C/N ratios 20 (Figure 9). These data suggest that there is mixed organic matter (e.g. from terrestrial and marine sources) in the Whitehill Formation.

The $\delta^{15}N$ values for the Prince Albert Formation range between 5.6 to 6.2‰, the Whitehill Formation between 7.7 to 10.1‰, and the Collingham Formation between 4.7 to 7.3‰. All three ranges are indicative of a marine source of organic matter (White, 2013). The Whitehill Formation has the highest $\delta^{15}N$ values, which could be a result of increased denitrification during periods of anoxia (Hoelke, 2011).

It is important to note that highly mature sediments have undergone both generation and expulsion of hydrocarbons. Since the generation of hydrocarbons is coupled to isotope fractionation, the interpretation of the presented data must be treated with caution.

Analysis of thermal maturity

Open pyrolysis and thermovaporization

Due to the high maturity of the samples, many of the chromatograms display peaks that are too small to be measured with precision. Instead, bulk parameters were calculated in open pyrolysis chromatograms: C1-C5, C6-C14 and C15+. As a result, most of the samples provide chromatograms that display low hydrocarbon generation, with peaks mostly within the C1-C5 region (Figure 10). Thermovaporization data were recorded by measuring the combined C1-C5 peaks and any following individual peaks: C6, Benzene and Toluene. Similar to pyrolysis, thermovaporization yields few significant peaks. According to this, no desorbable hydrocarbons are retained in the rock matrix.

Vitrinite reflectance

No fluorescing macerals were detected under UV illumination, likely due to the overmaturity of the rock samples. Reflected light microscopy, on the other

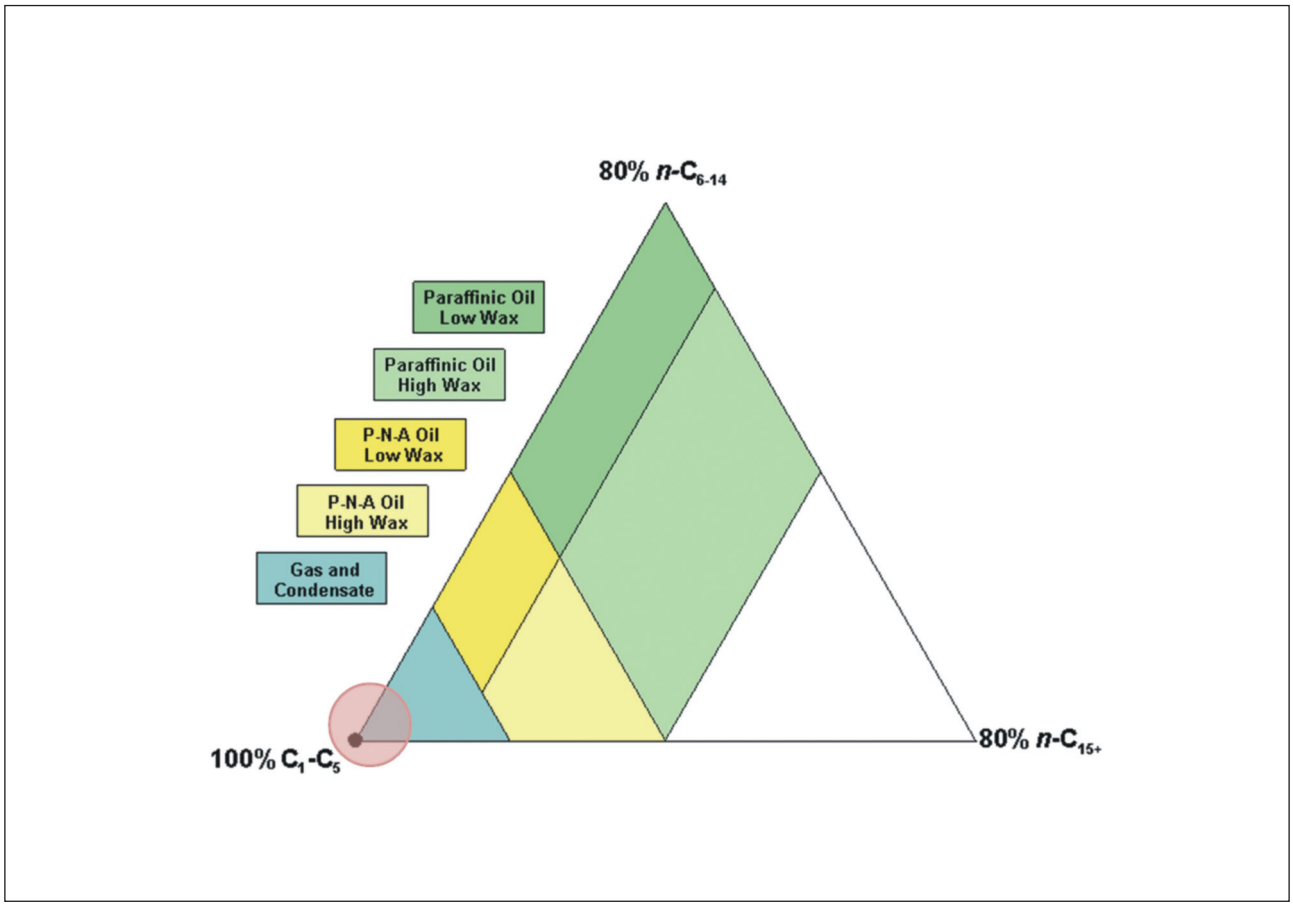

Figure 10. *Ternary diagram showing that all pyrolysis data from the study area are grouped in the C1-C5 category (based on Horsfield's Diagram 1989).*

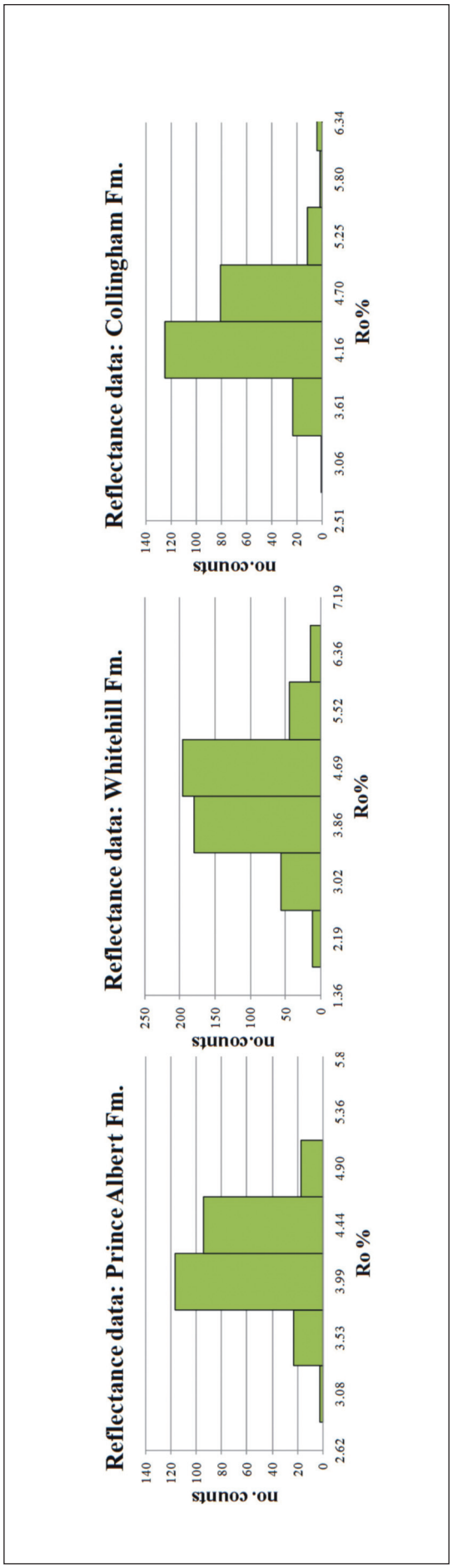

Figure 11. *Reflectance data R_o (representative of BR_o) plotted as histograms for the lower three formations of the Ecca Group. Note that reflectance values are similar for all three formations.*

hand, revealed that solid bitumen occurs in abundance and their grey values were measured and correlated with vitrinite reflectance. The reflectance measurements from the solid bitumen for all samples are on average ~4% BR_o, which classifies them as highly mature (Landis and Castanõ, 1995, Schoenherr et al., 2007) (Figure 11).

Porosity

Hg-intrusion porosimetry

Mercury intrusion porosimetry shows that meso- and macro-porosity is highest in the Whitehill Formation shales (1.35%), and in particular in the dolomite units (2.91%). SEM images show finely crystalline dolomite with intracrystalline porosity (Figure 12). The Prince Albert Formation has an average porosity of 0.53% and the Collingham Formation an average of 0.40% porosity.

Discussion and interpretation

The described general mineralogical and lithological composition of the rocks is consistent with those of previous investigators. Organic carbon content, thermal maturity, hydrocarbon content, porosity, and brittleness factors, as well as stable isotope data ($\delta^{13}C$ and $\delta^{15}N$) from shales of the lower Ecca Group, however, provide greater insight into the depositional environment of these rocks.

Rock fabric and facies interpretation

The presence of pyrite, phosphatic nodules, a miliolid foram fossil, rhythmite units and slumping features support the proposed hypothesis that the Prince Albert Formation was deposited from a continental shelf into an intercontinental basin (Smith et al., 1993). Sedimentary rocks have a TOC content of 0.37 weight % and contain both kerogen types II and III although thermal maturity factors and influence of sulfur content may have obscured these. $\delta^{13}C$ and $\delta^{15}N$ stable isotope data, C/N ratios and the presence of the miliolid fossil suggest a marine source of organic matter. However, we suggest that a mixed source of organic material is more plausible.

The black shale of the Whitehill Formation contains both framboidal and euhedral pyrite grains. The dolomite lenses and concretions occur randomly throughout the Whitehill Formation, but are most prevalent at the base of the formation. Rocks of the Whitehill Formation, being composed largely of illite, quartz and muscovite and containing bisaccated pollen of terrestrial origin, as well as a miliolid foram (possibly of marine origin) suggest that they formed in a mixed marine/terrestrial setting. Analytical data reveal an average TOC content of 4.5 weight %, and suggest that it contains type II kerogen, reflecting a high level of maturity. In addition $\delta^{13}C$ and $\delta^{15}N$ stable isotope data suggest a marine origin for the organic material, whilst C/N data imply that the source of organic material is of mixed origin (both type II and type III kerogen).

Thin section photomicrographs and SEM micrographs of the Collingham Formation reveal framboidal pyrite

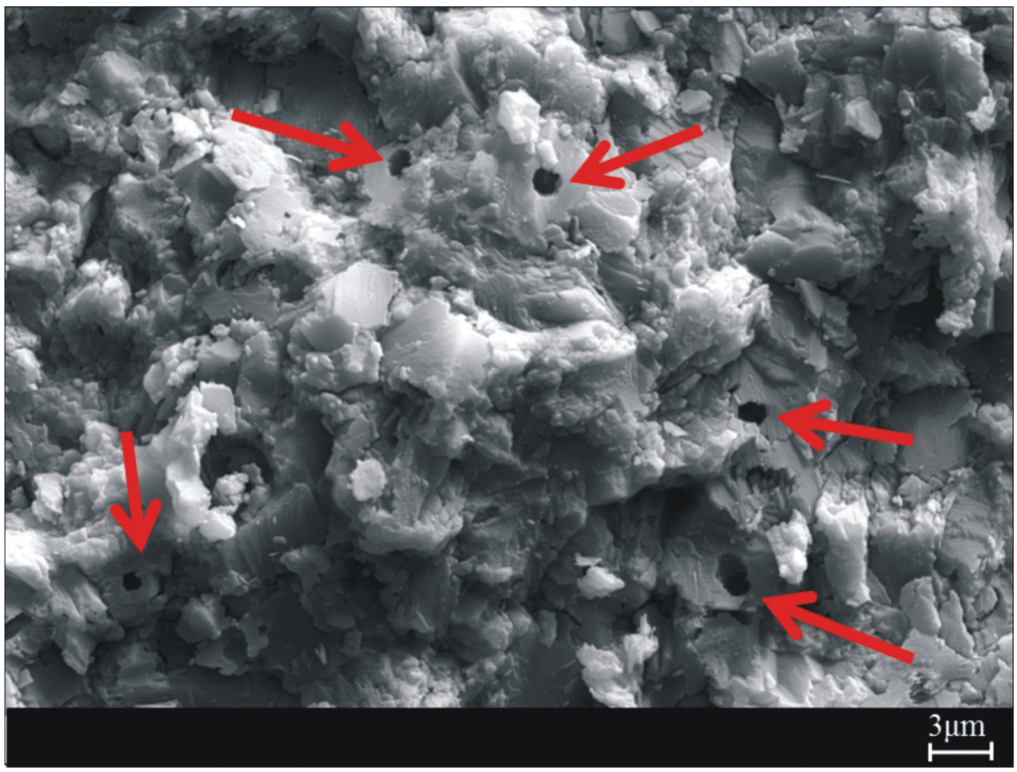

Figure 12. *A sample of dolomite (G011513) from the Whitehill Formation showing tightly packed and welded crystals of dolomite, with pores of secondary nature (arrowed).*

grains at the base of the formation near the contact with the Whitehill Formation. The Collingham Formation has the highest percentage of quartz (62%) relative to the lower two formations. As a result, the brittleness factor of the Collingham Formation is the highest. The TOC content of the Collingham Formation is low (0.62 weight %) and can be classified as type II kerogen. Similar to the Whitehill Formation, TOC/Rock Eval data are obscured by the effect of high thermal maturity, so determining kerogen type from these data is dubious. $\delta^{13}C$ and $\delta^{15}N$ stable isotope data, however, suggest that the organic material is from an aquatic (marine) source, and when comparing C/N versus $\delta^{13}C$, all samples fall within the marine algae zone with the exception of one (sample G011483) sampled near the top of the formation. Sample G011483 plots within the Whitehill Formation data range, suggesting mixed source of organic matter, which is consistent with terrestrial plant fragments already seen in the outcrop.

Palaeo-environmental conditions

Elemental ratios provide an indication of the oxic to anoxic variability, salinity and productivity of the palaeo-environment, but also about early diagenetic processes. Data from XRF, XRD and $\delta^{13}C$ and $\delta^{15}N$ stable isotopes, summarised in depth profile in Figure 6, are interpreted as follows:

The Whitehill Formation is high in clay minerals and relatively lower in silica content than the Collingham and Prince Albert Formations. The general SiO_2/Al_2O_3 ratio for shale is calculated to be between 2.01 and 4.04 (e.g., Campos Alvarez and Roser, 2006). Black shales of the Whitehill Formation match this closely, with a range of between 2.4 and 5.5. The 'high' SiO_2/Al_2O_3 value of 5.5 comes from one sample (G011491) near the contact with the Collingham Formation.

The Ba/Al_2O_3 ratio, a qualitative indicator of bio-productivity (Brumsack, 2006), appears to be the highest in the Collingham Formation and fluctuates within the Whitehill Formation. However, the detailed interpretation of the barite record in a sedimentary succession, especially in TOC-rich rocks, requires further studies, as barite also precipitates at the sulphate/ methane transition zone overlying black shales (Arndt et al., 2009). Importantly, the barite zone can move during ongoing sedimentation and is dependent on variables such as sedimentation rate (Arning et al., 2015). Mineralized phosphorous can also be used to follow ancient bio-productivity (e.g., Schoepfer et al., 2014); however and due to the above discussed items, a correlation is not seen between Ba/Al_2O_3 and P_2O_5/Al_2O_3, with the exception of the dolomite sample (G011513). The phosphorous signal is the highest in the Whitehill Formation possibly because phosphorous is

regenerated in the reductive Fe-cycle (Brumsack, 2006) that occurs in anoxic settings prevalent during the time of the Whitehill Formation deposition. Despite the detection of phosphate by XRF, phosphate minerals were not detected in XRD due to low contents, but do occur in the Whitehill Formation in other wells (Chere, 2015). Moreover, phosphorous has probably been absorbed into the clay minerals (Baioumy and Ismael, 2010).

Rb/K ratios provide an indication of fluctuations in palaeo-salinity of the basin. Rb/K values are higher in marine shales ($6*10^{-3}$) than those occurring in non-marine environments ($4*10^{-3}$) due to greater concentration of Rb in ocean waters (Scheffler et al., 2006). Rb/K ratios in the Prince Albert and the Whitehill formations (>$4*10^{-3}$) suggest a marine environment, whilst the Collingham Formation ($3.76*10^{-3}$ to $7.50*10^{-3}$) appears to fluctuate between marine and brackish conditions.

V/Cr ratios, similarly to Rb/K ratios, indicate a change in sedimentary conditions. V/Cr ratios can be used as a palaeo-redox indicator when it is found to correlate with TOC values. V/Cr ratios below 2 indicate oxic conditions during deposition, values between 2 and 4.25 ,represent a dysoxia, and ratios above 4.25 indicate anoxia (Scheffler et al., 2006). High V/Cr ratios (coupled with high Rb/K ratios) indicate that the Prince Albert Formation was deposited in an anoxic body with saline water. One deviation from this pattern is near the top of the Prince Albert Formation (sample G011518) where a rapid increase in Rb/K ratios is recorded. This is accompanied by a decrease in the V/Cr ratios, indicating a sudden influx of oxygenated water masses, possibly due to turbidity current activity. V/Cr ratios, highest in the Whitehill Formation, suggest an increase in anoxia conditions during this time. A general decrease in V/Cr ratios in shales of the Collingham Formation further strengthens the suggestion that increasingly oxygenated waters were present at that time. The above mentioned ratios in the mudrock units suggest a shift in sedimentary environmental conditions from the Prince Albert/ Whitehill formations to the Collingham Formation, where deposition of sediments changed from the central basin to more proximal regions. The progression to more brackish waters also suggests a shift to a more arid climate (Scheffler et al., 2006).

V/(V+Ni) ratios are used to determine palaeo-redox conditions and degrees of palaeo-productivity. V and Ni become highly enriched in sediment when algal matter encounters anaerobic conditions, shortly after, or during deposition (Brumsack, 2006). V/(V+Ni) values increase with increasing TOC content as a result of their diffusion into sediments under a slow sedimentation rate (Arthur and Sageman, 1994). V/(V+Ni) ratios for organic matter of around 0.84 indicate euxinic (anaerobic) conditions, between 0.54 and 0.84 for anoxic conditions, and between 0.46 and 0.60 for dysoxic (low in oxygen) conditions (Hatch and Leventhal, 1992). The V/(V+Ni) ratios within the Whitehill Formation are predominantly above 0.5, which indicates that it accumulated under anoxic conditions (Rimmer, 2004). The ratios indicate that the Prince Albert Formation accumulated primarily under euxinic conditions, and the Collingham Formation under more oxic conditions possibly due to rapid turbiditic input from shallower waters. One exception noted near the top of the Prince Albert Formation (G011518) shows a significant drop in V/(V+Ni) ratios (coincident with a reduction in the V/Cr ratio). This indicates an increase in the oxygen input at this horizon, probably due to short oxygenation of the bottom water during deposition.

Carbon-sulfur-iron relationships can also be used to determine the palaeo-redox conditions. Fe and S concentrations remain relatively stable, with only TOC being variable under conditions of thermal diagenesis (Ross and Bustin, 2009). Sedimentary rocks of the Whitehill Formation plot close to the anoxic zone, based on Ternary relationships between TOC-S-Fe to distinguish anoxic, dysoxic and oxic environments (Figure 8) (Ross and Bustin, 2009).

$\delta^{13}C$ and $\delta^{15}N$ values shed light on the origin of the organic matter. In the case of the Whitehill Formation, stable carbon isotope values suggest a marine source, (based on interpretations by White, 2013), and elevated values of $\delta^{15}N$ probably reflect denitrification, resulting from anoxic conditions (c.f. Hoelke, 2011).

Sulfides, predominantly in the form of pyrite framboids and larger euhedral cubic crystals occur in all three of the formations, but dominantly in the Whitehill Formation. They are interpreted to be both authigenic and diagenetic in origin, suggesting prolonged sulfate reduction processes in the mudrock units. Additionally, the presence of framboidal pyrite of uniform grain size indicates microbial activity, and, coupled with elevated concentrations of barium and phosphorous in carbonate rocks, suggests an anoxic bottom water caused by high palaeoproductivity during which pyrite already formed in the water column.

Dolomite concretions and lenses near the base of the Whitehill Formation are laminated and exhibit a physical texture that resembles microbial mats and/or stomatolite-like features. In thin section the dolomite has an aphanitic texture and under the SEM spherical 'holes' are enclosed within the dolomite crystals. These may be moulds from remnant bacteria and have consequently enhanced the porosity, but not the permeability. According to Perri and Tucker (2013), stromatolites have almost complete dolomite mineralogy, and they propose that sulphate-reducing bacteria caused the precipitation of dolomite from microbial mats. Dolomites of the Whitehill Formation may have such an origin, but this interpretation was not verified in this study. If this interpretation was applied here then carbonate rocks would have an origin in shallow, pre-tidal environments – a setting that does not conform to a proposed inland anoxic ocean. Dolomite precipitation is, however, well-known from sulfate reduction in TOC-rich sediments (Macquaker et al., 2014).

Table 1. The Whitehill shale compared with the Barnett and Marcellus shales (data from Bruner and Smosna (2011), Hoelke J (2011) and Decker and Marot (2012)).

Property	Barnett (Mississippian shale Fort Worth Basin, USA)	Marcellus (Devonian Shale, Appalachian Basin USA)	Whitehill (Permian Shale, South Eastern Karoo Basin, Greystone area, RSA)
Mineral (%)			
Quartz	35 to 50	10 to 60	13 to 55
Clays (illite)	10 to 50	10 to 35	5 to 29
Calcite, dolomite, siderite	0 to 30	3 to 50	3 to 62
Feldspars	7	0 to 4	0 to 24
Pyrite	5	5 to 13	1 to 16
Phosphate, gypsum	trace	trace	trace
Mica	0	5 to 30	3 to 22
Porosity (%)	3 to 6	3 to 6	2.90 (including dolomite), 0.83 (excluding dolomite)
Vitrinite reflectance (R_o)	1.2 (max 1.9)	1.6 (max 3.5)	4
Tmax	465°C	475°C	563°C
TOC (%)	2 to 6	1 to 10	0.7 to 8.15
Kerogen type	Type II (minor admixture of type III)	Type II (mixture of type III)	Mixture of type II and type III
Estimated size of shale-gas play	23 310 km^2	129 499 km^2	155000km^2 to 183 000km^2
Thickness of formation	107m	15m	~28m
Estimated Potential yield	2.5 bcf to 40tcf	50 to 900tcf	between 32tcf and 485tcf

Data from this study suggest that the palaeo-depositional environment was marine during the deposition of sediments that comprise the Prince Albert and Whitehill Formation. This interpretation is, however, in contrast with interpretations by Faure and Cole (1999) for the Whitehill Formation in the Kimberley area, who propose that the depositional environment was lacustrine with fresh to brackish water, based on stable isotope data from ^{13}C, ^{34}S and ^{18}O, and $C_{(org)}/S$ ratios.

Thermal maturity

Samples of core analysed in this study occur in the CFB front - a region where the Karoo Supergroup strata are deformed by internal shortening, folding and faulting. In the study area rocks of the lower Karoo Supergroup crop out some 100 km south of the northernmost deformation front of the fold belt, and 5 km north of strata of the Cape Supergroup. The Whitehill Formation in particular is highly deformed, often with a distinct cleavage, is veined, and has been interpreted as a "décollement" zone (Lindeque et al., 2007; Kingsley, 1981). Quartz-calcite precipitation in veins during the Cape Orogeny may record the deformation that took place at the CFB tectonic front. In the region between Prince Albert and Laingsburg in the Western Cape, quartz-calcite geothermometry of the veins in the Prince Albert Formation reveal trapping temperatures between 230 to 260°C at 2 to 3 kbar. The research in this area suggests devolatilization during low grade (up to lower greenschist) metamorphism (Egle, 1996 and Egle et al., 1998; Craddock et al., 2008). Core samples from the Greystone area analysed in this study show similar extensive calcite veining along bedding planes, cleavages and joint fractures of the Prince Albert Formation and it can be expected that they share similar trapping temperatures.

It can be assumed that the maturation of the Ecca Group in the Greystone study area has been brought about through tectonic burial and metamorphism of the CFB. This is revealed via data from Rock Eval pyrolysis, vitrinite reflectance, thermovaporization and open pyrolysis techniques:

Vitrinite reflectance testing showed that no original macerals could be identified in the samples; instead, solid bitumen was discovered. Bitumen reflectance values were found to be high, with an average BR_o of 4%, which indicates that the rocks are over-mature. The presence of solid bitumen is an indicator of hydrocarbon generation and migration within the rock and is a by-product that forms when oil thermally cracks to form light hydrocarbons. Due to high temperatures, bitumen corresponds to very low HI values (<80mg HC/g TOC) and high Tmax values (>460 °C) (Schoenherr et al., 2007). In a study by Branch et al., (2007) vitrinite reflectance was performed on four samples from Soekor hole SA 1/66 located some 100 km from the CFB tectonic front. One sample from the Whitehill Formation was found to contain solid bitumen. The remaining three samples were taken from the Prince Albert Formation and were found to contain graphitic particles as well as vitrinite.

Rock Eval pyrolysis in this study showed very low HI values (<80mg HC/g TOC) for all formations (lowest values were seen in the Whitehill Formation). A possible reason for such low values is that oil that is released from kerogen may have been adsorbed onto the surface

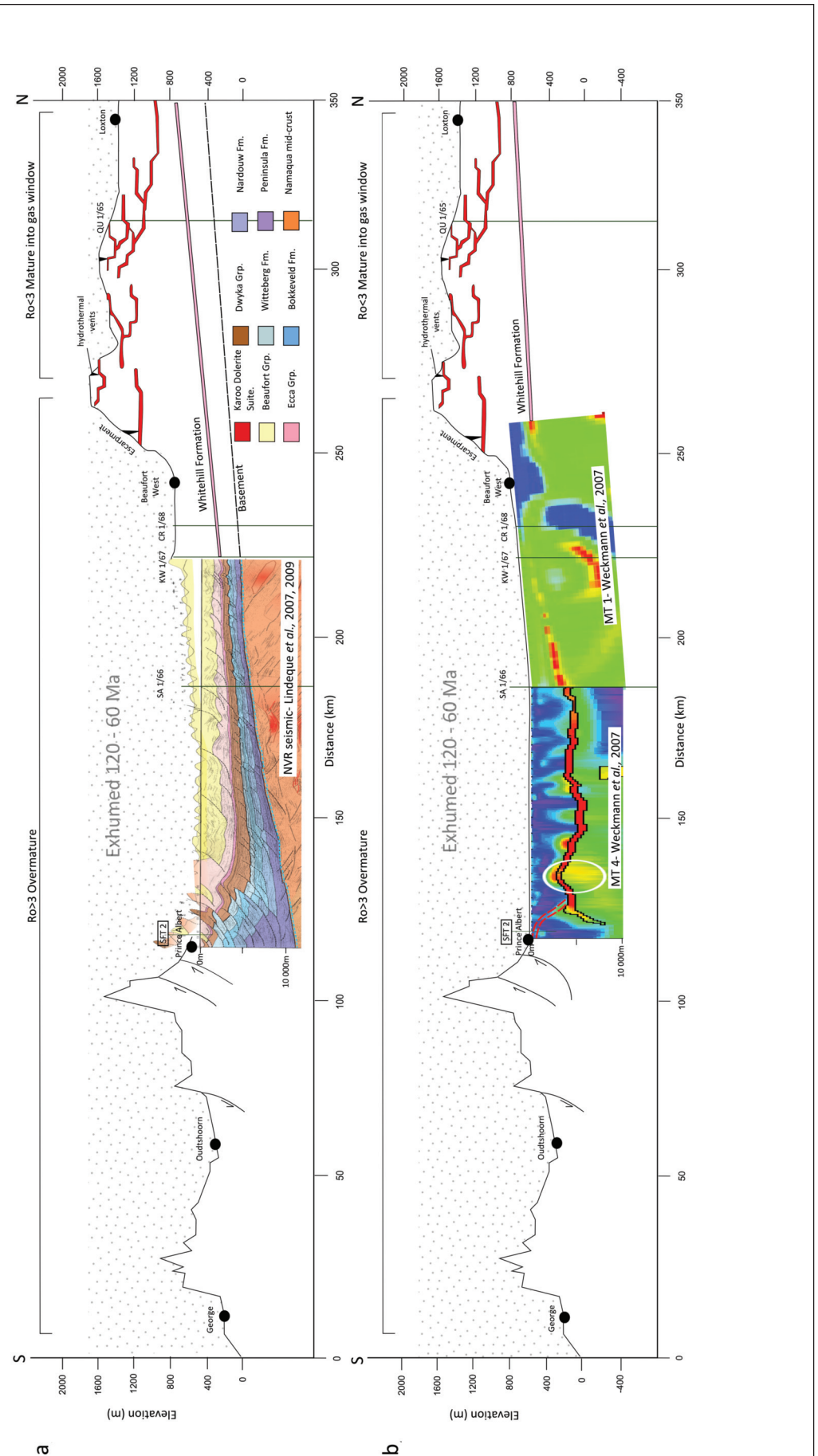

Figure 13 *(**a**) Cross section using geological and geophysical data from Tinker et al., (2008) and Lindeque et al, (2007;2011) (**b**) Cross section using data from Tinker et al., (2008) and Weckmann et al., (2007), which is projected westerly along strike from the north-south profile centred on Jansenville.*

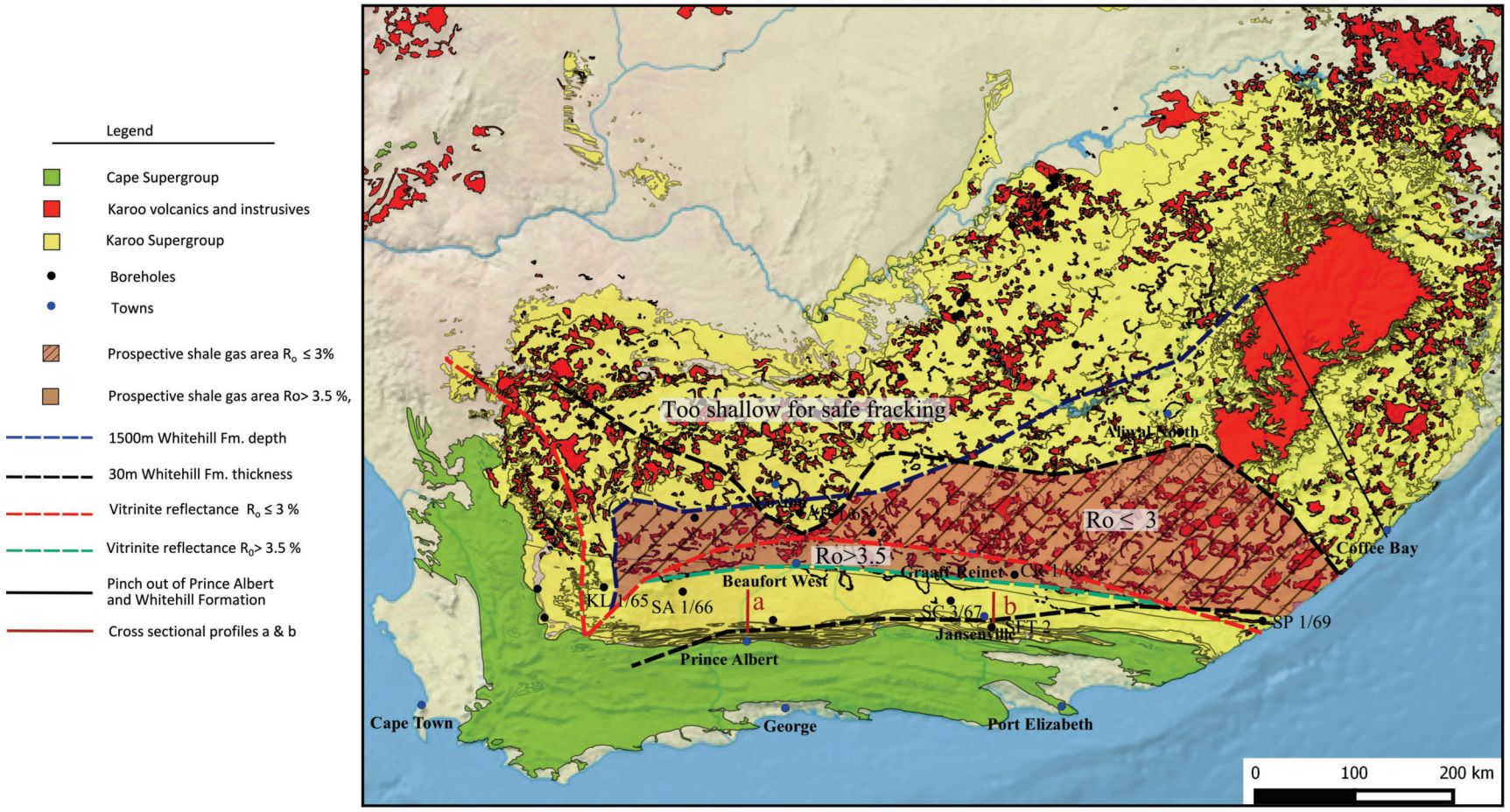

Figure 14. *Parameters for maturity (vitrinite reflectance (R_o) ≤3% and >3.5% and depths and thickness of the Whitehill Formation are used to outline the prospective shale gas areas. A gas recovery value of 30% and a 50% success factor is considered and the potential recoverable free gas in the Karoo Basin is estimated to be between 19-23 tcf.*

of the clay minerals. This would reduce the S2 peak, and as a consequence reduce the HI values. This effect has been seen in illite and montmorillonite (Hartwig, 2009). The low HI values of the Whitehill Formation are likely therefore to be due to a combination of high clay content, high sulfur content, and the presence of solid bitumen.

The Tmax values for the Prince Albert, Whitehill and Collingham Formations range from 460 to 572 °C, which characterises the sedimentary rocks as late- mature to post-mature. Only a few samples yielded Tmax values that classify them as immature. The latter occurs mostly in the Collingham Formation, with one sample from the gradational contact with the lower Dwyka Group. On the Van Krevelen plot these data are coincident with the bitumen reflectance data that shows these rocks can be grouped into the over-mature zone and in the dry gas window.

Pyrolysis-GC and thermovaporization analysis show poor hydrocarbon generation and detected mostly short chain hydrocarbons within the C1 to C5 range. In Pyrolysis-GC only one sample from each of the Whitehill and Collingham Formations produced hydrocarbons from all three ranges (C1 to C5, C6 to C14, C15+). In thermovaporization analysis only one sample from the Whitehill Formation produced peaks of C1 to C5, C6, benzene and toluene. This overall poor hydrocarbon generation is also a reflection of highly over-mature rocks.

The lower Ecca Group as a potential shale gas reservoir

Exploitable gas-bearing shales generally have the following characteristics: 1) high organic richness, 2) secondary cracking of kerogen and retention of oil, 3) retention of oil for cracking to gas by adsorption, 4) porosity resulting from decomposition of organic matter, 5) mineral induced brittleness. The Whitehill Formation complies with most of these characteristics and is therefore the most favourable formation of the lower Ecca Group that has the potential to host viable gas deposits. The Whitehill Formation, with its high TOC content (4.5 weight %), was deposited under suitable anoxic quiescent bottom water conditions to allow for the preservation of organic matter. The presence of solid bitumen suggests that thermal cracking processes took place, probably as a result of thermal overprinting during the Cape Orogeny. The mineralogy of the shale suggests suitable brittleness due to high quartz, calcite and dolomite content. Although this study does not provide more information on organic porosity, nor the adsorption qualities of the shale, it is clear that the samples evaluated are highly affected by their location relative to the CFB. The position of the study area within the CFB and the shallow depth of the borehole (100 to 300 m) have affected the ability of the shale to retain gas. The fact that very little hydrocarbons remain in these rocks indicates that most of the gas, which potentially may have been generated, was lost during thermal overprinting. In future samples should be collected from greater depths in the basin (2 to 4 km depths) and farther away from the influence of the CFB, to test the retention potential of gas within these shales.

A chart comparing the characterisitics of the Karoo Basin with those of two well-known shale gas yielding basins in the USA, i.e. the Mississippian Barnett Shale (Fort Worth Basin) and the Devonian shales of the Marcellus Basin, is shown in Table 1. The Barnett and Marcellus shales were used for comparison due to the large amount of information available from these basins. The Whitehill Formation is very similar to these well-known examples when comparing thermal maturity, quartz content (favourable for hydraulic fracturing), TOC content and the mixture of type II and type III kerogen. Shales of the Whitehill Formation are, however, more mature than those of the Marcellus Basin (where this is well away from the tectonic front of the Appalachians) and the Barnett shales, probably as a result of their position close to the tectonic front of the CFB. One exception is that shales of the Whitehill Formation have lower porosity values then those of the USA examples. This, however, could be a function of the fact that mercury intrusion only measures the meso- and macro-porosity and if micro-pores were included, the porosity figures may yield higher values.

The abovementioned characteristics of shales of the Whitehill Formation suggest that they have the potential for holding significant amounts of gas.

Assessing the shale-gas potential of the Karoo Basin

The following parameters are considered to be essential by limiting factors in the calculation of hydrocarbon reserves of the Whitehill Formation in the Karoo Basin: the maturity of sedimentary rocks, the thickness and depth of the formation; and thickness of dolerite intrusions. The database used in the calculations was extracted from this study, as well as from boreholes drilled during 1965 by Soekor (Petroleum Agency of South Africa (PASA), see Rowsell and De Swart, 1976; Cole 2014). Dolerite thicknesses were obtained from published 1:250 000 geological maps (Toerien, 1991).

Based on recent studies in the area (Weckmann et al., 2007; Tinker et al., 2008 and Lindeque et al., 2007; 2011) two cross sections, extending from Loxton to George through the middle part of the Karoo basin, were constructed in order to calculate the depth configuration of the Karoo Supergroup. The first section (Figure 13a) is a compilation of geological and geophysical data from Tinker et al. (2008) and Lindeque et al. (2007; 2011), whereas the second section (Figure 13b) shows an interpretation using data from Tinker et al., (2008) and magnetotelluric (MT) data from Weckmann et al. (2007). Cross section Figure 13b is drawn using MT1 data from a north-south profile between Prince Albert and Fraserburg and MT4 data, which is projected westerly along strike from the north-south profile centred on Jansenville.

Based on the abovementioned data, a map was constructed (Figure 14) that summarizes the shale parameters and the areal extent most favourable to explore for gas in the Karoo. It is assumed that the gas present is methane, and until hydraulic fracturing is undertaken and actual yields and gas composition ascertained, our calculated figures are to be interpreted with caution. The area is delineated on its southern side by two lines just north of Beaufort West and Graaf-Reinet and on towards East London according to vitrinite reflectance data (R_o 3 and R_o>3.5). This reflects the tectonic front of the CFB. Its northern extremity is delineated by the 30 metre isopach of the Whitehill Formation. The prospective area thus defined measures 92 170 km^2 to 78 726 km^2. Using an average thickness of 30 m for the Whitehill Formation, a porosity value of 1.57%, a gas recovery value of 30% and a 50% success factor (Decker, personal communication, 2014), the recoverable reserves amount to 19 to 23 tcf of available free gas. This calculation does not include the adsorbed gas or micro-porosity, which would result in a higher estimate of gas present in the Whitehill Formation. Cole (2014) similarly calculated a possible resource of 18.5 tcf based, however, on a smaller prospective area; R_0<3.5 and assuming dolerite intrusions in less than 20% of the succession.

Conclusions

Samples of fresh core from boreholes drilled through lower Ecca Group rocks near Jansenville, analysed for their petrographic, geochemical and petro-physical properties, indicate the following:

- That the shales of the Prince Albert and Whitehill formations were deposited in an anoxic environment, in contrast to those of the overlying Collingham Formation, which formed in shallower oxygenated conditions.
- That the palaeo-environmental setting for the basin was likely marine, becoming increasingly lacustrine, with fresh to brackish conditions prevailing by the Collingham Formation with deposition of mixed (terrestrial and marine) organic matter.
- That the Whitehill Formation in particular is rich in TOC, and thus a favourable source unit for potential gas.

Petrophysical analyses further indicate that properties such as brittleness and porosity of the Whitehill Formation, although not as suitable as the under- and over-lying formations, would facilitate hydraulic fracturing and extraction of gas from these rocks.

The presence of bitumen, as well as the very small proportions of hydrocarbons in the shales, show that rocks in the study area are over-mature, and do not contain any significant quantities of natural gas.

Characteristic properties of the Whitehill Formation as a suitable shale gas host compare favourably with those of currently exploited gas fields in the United States. The Whitehill Formation therefore, in the context of the Karoo Basin, remains an attractive target as a potentially suitable shale gas resource, but only if explored in the region away from the influence of the Cape Fold Belt.

Acknowledgments

We would like to thank the GFZ (Potsdam, Germany), NRF and Inkaba yeAfrica for funding to carry out this research. We also thank John Hancox and Doug Cole for thorough reviews from which we benefited. This is Inkaba yeAfrica contribution number 117; and AEON contribution number 138.

References

Aarnes, I., Svensen, H., Connolly, J.A.D. and Podladchikov, Y.Y., 2010. How contact metamorphism can trigger global climate changes: Modeling gas generation around igneous sills in sedimentary basins. Geochimica et Cosmochimica Acta, 74, 7179-7195.

Aarnes I., Svensen, H., Polteau, S. and Planke, S., 2011. Contact metamorphic devolatilization of shales in the Karoo Basin, South Africa, and the effects of multiple sill intrusions. Chemical Geology, 281, 181-194.

Arthur, M.A. and Sageman, B.B., 1994. Marine Black Shales: Depositional Mechanisms and Environments of Ancient Deposits. Earth and Planetary Science Letters, 22, 499-551.

Arndt, S., Hetzel, A. and Brumsack, H-J., 2009. Evolution of organic matter degradation in the Cretaceous black shales inferred from authigenic barite: A reaction-transport model. Geochimica et Cosmochimica, 73, 2000-2022.

Arning, E.T., Gaucher, E.C., van Berk, W. and Schulz, H-M., 2015. Hydrogeochemical models locating sulfate-methane transition zone in marine sediments overlying black shales: a new tool to locate biogenic methane? Marine and Petroleum Geology, 59, 563-574

Baceta, J.I. and Nunez-Betelu, L., 1994. Basics and Application of Rock-Eval/TOC Pyrolysis: an example from the uppermost Paleocene/lowermost Eocene. In: The Basque Basin, Western Pyrenees. Department of Geology and Geophysics, The University of Calgary, Ciencias Naturales-Natur Zientziak, 46, 43-62.

Baioumy, H.M. and Ismael, I.S., 2010. Factors controlling the compositional variations among the marine and non-marine black shales from Egypt. International Journal of Coal Geology, 83, 35-45.

Bangert, B., Stollhofen, H., Lorenz, V. and Armstrong, R., 1999. The geochronology and significance of ash-fall tuffs in the glaciogenic Carboniferous-Permian Dwyka Group of Namibia and South Africa. Journal of African Earth Sciences, 29(1), 33-49.

Burgess, S.D., Bowring, S.A., Fleming, H. and Elliot, D.H., 2015. High-precision geochronology links the Ferrar large igneous province with early-Jurassic ocean anoxia and biotic crisis. Earth and Planetary Science Letters, 415, 90-99.

Booth, P.W.K. and Shone, R.W., 1999. Complex thrusting at Uniondale, eastern sector of the Cape fold belt, Republic of South Africa: structural evidence for the need to revise the lithostratigraphy. Journal of African Earth Sciences, 29, 125-133.

Booth, P.W.K. and Shone, R.W., 2002. A review of thrust faulting in the Eastern Cape Fold Belt, South Africa, and the implications for current lithostratigraphic interpretation of the Cape Supergroup. Journal of African Earth Sciences, 34, 179-190.

Booth, P.W.K. and Goedhart, M.L., 2014. Thrust faulting in the northernmost foreland zone of the Cape Fold Belt, Fort Beaufort, Eastern Cape, South Africa. South African Journal of Geology, 117, 301-315.

Branch, T., Ritter, O., Weckman, U., Sachsenhofer, R. and Schilling, F., 2007. The Whitehill Formation- a high conductivity marker horizon in the Karoo Basin. South African Journal of Geology, 110, 465-476.

Brandt, A.R., Heath, E.A., Kort, F., O'Sullivan, G., Pétron, S.M., Jordaan, P., Tans, J., Wilcox, A.M. ,Gopstein, D., Arent, S., Wofsy, N.J., Brown, R., Bradley, G.D., Stucky, D., Eardley, R. and Harris, R., 2014. Methane Leaks from North American Natural Gas Systems. Science, 343, 733-735.

Brumsack, H.J., 2006. The trace metal content of recent organic carbon-rich sediments: Implication for Cretaceous black shale formation. Palaeogeography, Palaeoclimatology, Palaeoecology, 232, 344-361.

Bruner, K.R. and Smosna, R., 2011. A Comparative Study of the Mississippian Barnett Shale, Fort Worth Basin, and Devonian Marcellus Shale, Appalachian Basin. U.S. Department of Energy (DOE). National Energy Technology Laboratory (NETL), 118p.

Campos Alvarez, N.O. and Roser, B.P., 2006. Geochemistry of black shale from the Lower Cretaceous Paja Formation, Eastern Cordillera, Columbia: Source weathering, provenance and tectonic setting. Journal of South American Earth Sciences, 23, 271-289.

Catuneanu, O., Wopfner, H., Eriksson, P.G., Cairncross, B., Rubidge, B.S., Smith R.M.H. and Hnacox P.J., 2005. The Karoo basins of south-central Africa. Journal of African Earth Sciences, 43, 211-253.

CCA – Council of Canadian Academies, 2014. Environmental Impacts of Shale Gas Extraction in Canada. Ottawa (ON): The Expert Panel on Harnessing Science and Technology to Understand the Environmental Impacts of Shale Gas Extraction, Council of Canadian Academies, 262p.

Chere, 2015. Sedimentological and geochemical investigations on boreholes cores of the Lower Ecca Group black shales, for their gas potential - Karoo Basin, South Africa. Unpublished Master Thesis, Nelson Mandela Metropolitan University, South Africa, 175p.

Cloetingh, S., Lankreijer, A., de Wit, M.J. and Martinez, I., 1992. Subsidence history analyses and forward modelling of the Cape and Karoo Supergroups. In: M.J. De Wit and I.D.G. Ransome (Editors). Inversion Tectonics of the Cape Fold Belt, Karoo and Cretaceous Basins of Southern Africa, Balkema, Rotterdam, Netherlands, 239-248.

Cole, D.I., 1992. Evolution and development of the Karoo Basin. In: M.J. De Wit and I.D.G. Ransome, (Editors). Inversion Tectonics of the Cape Fold Belt, Karoo and Cretaceous Basins of Southern Africa., Balkema, Rotterdam, Netherlands, 87-99.

Cole, D.I., 2005. Prince Albert Formation pp. 8-33–8-36, In: M.R. Johnson, (Editor). Catalogue of South African Lithostratigraphic Units. South African Committee for Stratigraphy, Volume 8, Government Printer, Pretoria, 43p.

Cole, D.I., 2014. Geology of Karoo Shale Gas and how this can Influence Economic Gas Recovery. Presentation, Gas – The Game Changer for Southern Africa?!. Fossil Fuel Foundation, Glen Hove, Johannesburg, 21 May 2014, Abstracts, 11-12.

Cook, P., Beck, V., Brereton, D., Clark, R., Fisher, B., Kentish, S., Toomey, J. and Williams, J., 2013. Engineering energy: unconventional gas production. Report for the Australian Council of Learned Academies, 250p.

Craddock, J.P., Alex W., McKiernan, A.W. and de Wit, M.J., 2008. Calcite twin analysis in syntectonic calcite, Cape Fold Belt, South Africa: Implications for fold and cleavage formation within a shallow thrust front. Journal of Structural Geology, 29, 1100-1113.

De Wit, M.J. and Ransome, I.G.D., 1992. Regional inversion tectonics along the southern margin of Gondwana. In: M.J. De Wit and I.G.D. Ransome (Editors), Inversion tectonics of the Cape Fold Belt, Karoo and Cretaceous Basins of Southern Africa. Balkema, Rotterdam, Netherlands, 15-20.

Dean, W.E. and Arthur, M.A., 1989. Iron-sufur-carbon relationships in organic-carbon-rich sequences I: Cretaceous western interior seaway. American Journal of Science, 289, 708-473.

Decker, J. and Marot, J., 2012. Investigation of hydraulic fracturing in the Karoo of South Africa. Annexure A, Resource Assessment, Petroleum Agency SA. Available at: <http://www.dmr.gov.za/publications/viewdownload/ 182/854.html> (viewed 01-11-13).

Decker, J.E., Niedermann, S. and de Wit, M.J., 2013. Climatically influenced denudation rates of the southern African plateau: Clues to solving a geomorphic paradox. Geomorphology, 190, 48-60.

Duncan, R.A., Hooper, P.R., Rehacek, J. and Duncan, A.R., 1997. The timing and duration of the Karoo igneous event, Southern Gondwana. Journal of Geophysical Research, 102, 127-138.

Egle, S., 1996. Paleohydrology of the Cape Fold Belt and Karoo Basin, South Africa. Unpublished PhD thesis, University of Cape Town, South Africa, 155p.

Egle, S., de Wit, M.J. and Hoernes, S., 1998. Gondwana fluids and subsurface palaeohydrology of the Cape Fold Belt and the Karoo Basin, South Africa. Journal of African Earth Sciences, 27, 63-64.

Ensor, L., 10 October 2013. 'Cabinet gives Green light to draft fracking rules'. Business Day Live. Available at: <http://www.bdlive.co.za/business/energy/2013/10/10/cabinet-gives-green-light-to-draft-fracking-rules> (viewed 11-11-13).

Faure, K. and Cole, D., 1999. Geochemical evidence for lacustrine microbial blooms in the vast Permian Main Karoo, Parana, Falkland Islands and Haub basins of southwestern Gondwana. Palaeogeography Palaeoclimatology Palaeoecology, 152, 189-213.

Fildani, A., Weislogel, A., Drinkwater, N.J., McHargue, T., Tankard, A. and Woodens, J., 2009. U-Pb zircon ages from the southwestern Karoo Basin, South Africa-Implications for the Permian-Triassic boundary. Geology, 37, 719-722.

Geel, C., 2014. Shale gas characteristics of Permian black shales in the Ecca Group, Near Jansenville, Eastern Cape, South Africa. Master Thesis, Nelson Mandela Metropolitan University, South Africa, 163p.

Geel, C., Schulz, H.M., Booth, P., de Wit, M. and Horsfield, B., 2013. Shale gas characteristics of Permian black shales in South Africa: results from recent drilling in the Ecca Group (Eastern Cape). Energy Procedia, 40, 256-265.

Giesche, H., 2006. Mercury Porosimetry: A General (Practical) Overview. Particle & Particle Systems Characterization, 23, 1-11.

Hälbich, I.W., 1993. (Compiler) Global Geoscience Transect 9. The Cape Fold Belt - Agulhas Bank transect across Gondwana Suture, Southern Africa. American Geophysical Union Special Publication, 202, 18.

Hansma, J., Eric Tohver, E., Jourdan, F., Schrank, C. and David Adams, D., 2015. The timing of the Cape Orogeny: New 40Ar/39Ar age constraints on deformation and cooling of the Cape Fold Belt, South Africa. Gondwana Research, in Press. doi: 10.1016/j.gr.2015.02.005

Hartwig, A., 2009. Upper Carboniferous and Upper Permian Black Shales in Northeast Germany: Investigations of sedimentary and organic material regarding their shale gas characteristics. Diplomarbeit, Technische Universität Berlin. Institut für angewandte geowiseenschaften fachberiech explorations geologie, 135p.

Hatch, J.R. and Leventhal, J.S., 1992. Relationship between inferred redox potential of the depositional environment and geochemistry of the Upper Pennsylvanian(Missourian) stark shale member of the Dennis Limestone, Wabaunsee County, Kansas, USA. Chemical Geology, 99, 65-82.

Hoelke, J.D., 2011. Chemostratigraphy and Paleoceanography of the Mississippian Barnett Formation, Southern Fort Worth Basin, Texas, USA. Master of Science Degree, University of Texas, Arlington, 96p.

Horsfield, B., 1989. Practical criteria for classifying kerogens: Some observations from pyrolysis gas chromatography. Geochimica et Cosmochimica Acta, 53, 81-901.

Isabell, J.L., Cole, D.I. and Catuneanu, O., 2008. Carboniferous- Permian glaciation in the main Karoo Basin, South Africa: Stratigraphic, depositional controls and glacial dynamics. In: C.R. Fielding, T.D. Frank and J. L.Isabell (Editors). Resolving the Late Palaeozoic Age in Time and Space. Geological Society of America, Special Paper, 441, 71-82.

Jacob, H., 1989. Classification, structure, genesis and practical importance of natural solid oil bitumen (migrabitumen). International Journal of Coal Geology, 11, 65-79.

Jarvie, M.D., Hill, R.J., Ruble, T.E. and Pollastro, R.M., 2007. Unconventional shale-gas systems: The Mississippian Barnett Shale of north-central Texas as one model for the thermogenic shale-gas assessment. AAPG Bulletin, 91, 475-499.

Johnson, M.R., Van Vuuren, C.J., Visser, J.N.J., Cole, D.I., Wickens, H. de V., Christie, A.D.M., Roberts, D.L. and Brandl, G., 2006. Sedimentary rocks of the Karoo Supergroup. In: M.R. Johnson, C.R., Anhaeusser and R.J. Thomas (Editors). The Geology of South Africa. Geological Society of South Africa/Council for Geoscience, 461-499.

Kingsley, C.S., 1977. Stratigraphy and Sedimentology of the Ecca Group in the Eastern Cape Province, South Africa. PhD thesis, University of Port Elizabeth, Port Elizabeth, 290p.

Kingsley, C.S., 1981. A Composite Submarine Fan-Delta-Fluvial Model for the Ecca and Lower Beaufort Groups of Permian Age in the Eastern Cape Province, South Africa. Transactions of the Geological Society of South Africa, 84, 27-40.

Kuuskraa, V., Stevens, S., Van Leeuwen, T. and Moodhe, K., 2011. World shale gas resources: An initial assessment. Prepared for: United States Energy Information Administration. World Shale Gas Resources: An Intital Assessment of 14 Regions Outside the United States. Available at: <http://www.eia.doe.gov/analysis/studies/worldshalegas> (viewed 04-04-13).

Lanci, L., Tohver, E., Wilson, A. and Flint, S., 2013. Upper Permian magnetic stratigraphy of the lower Beaufort Group, Karoo Basin. Earth and Planetary Science Letters, 375, 123-134.

Landis, C.R. and Castanõ, J.R., 1995. Maturation and bulk chemical properties of a suite of solid hydrocarbons. Organic Geochemistry, 22, 137-149.

Lindeque, A., Ryberg, T., Stankiewicz, J., Weber, M. and de Wit, M., 2007. Deep Crustal Reflection Experiment across the Southern Karoo Basin, South Africa. South African Journal of Geology, 110, 419-438.

Lindeque, A., De Wit, M.J., Ryberg, T., Weber, M. and Chevallier, L., 2011. Deep crustal profile across the southern Karoo Basin and Beattie magnetic anomaly, South Africa: An integrated interpretation with tectonic implications. South African Journal of Geology, 114, 265-292.

Lock, B.E., 1980. Flat-plate subdcution and the Cape Fold Belt of South Africa. Geology, 8, 35-39.

Linol, B., de Wit, M.J., Milani, E. J., Guillocheau, F. and Scherer, C., 2015. New Regional Correlations Between the Congo, Parana´ and Cape-Karoo Basins of Southwest Gondwana In: M.J. de Wit et al. (eds.), Geology and Resource Potential of the Congo Basin, Regional Geology. Springer-Verlag Berlin, Germany, 642p.

Macmullin, A., 28 February 2013. 'Treasury to introduce carbon tax, effective from 2015-Gordhan'. Business Day live. Available at: <http://www.bdlive.co.za/national/science/2013/02/27/treasury-to-introduce-carbon-tax-effective-from-2015—gordhan > (viewed 17-12-13).

Macquaker, J.H.S., Taylor, K.G., Keller, M. and Polya, D., 2014. Compositional controls on early diagenetic pathways in fine-grained sedimentary rocks: Implications for predicting unconventional reservior attributes of mudstones. American Association of Petroleum Geologists, (AAPG Bulletin), 93, 587-603.

Maré. L.P., De Kock, M.O., Cairncross, B. and Mouri, H., 2014. Application of magnetic geothermometeres in sedimentary basins: An example from the Western Karoo Basin, South Africa. South African Journal of Geology, 117, 1-14.

Martin, J.P., Hill, D.G., Lombardi, T.E. and Nyahay, R.E., 2008. 'A Primer on New York's Gas Shales,' New York State Geological Association: Field Trip Guidebook-80th Annual meeting, Lake George, NY, NYSGA, 2008, 32p.

Mauter, M.S., Alvarez, P.J.J., Burton, A., Cafaro, D.C., Chen, W., Gregory, K.B., Jiang, Li, Q., Pittock, J., Reible, D. and Schnoor, J.L., 2014. Regional Variation in Water-Related Impacts of Shale Gas Development and Implications for Emerging International Plays. Environmental Science and Technology, 48, 8298-8306.

McKay, M.P., Weislogel, A.L., Fildani, A., Rufus L., Brunt, R.L., David M. Hodgson, D.M. and Flint, S.S., 2015. U-PB zircon tuff geochronology from the Karoo Basin, South Africa: implications of zircon recycling on stratigraphic age controls. International Geology Review, 57, 393-410.

Meyer, P.A., 1994. Preservation of elemental and isotopic source identification of sedimentary organic matter. Chemical Geology, 144, 289-302.

Milani, E.J. and de Wit, M.J., 2008. Correlations between the classic Paraná and Cape Karoo sequences of South America and southern Africa and their basin infills flanking the Gondwanides: du Toit revisited. In: R.J. Pankurst, R.A.J. Trouw, B.B. Brito Neves and M.J. de Wit (Editors). West Gondwana: Pre-Cenozoic Correlations across the South Atlantic Region. The Geological Society, London, Special Publications, 294, 319-342.

Paton, D.A., Macdonald, D.I.M. and Underhill, J.R., 2006. Applicability of thin or thick skinned structural models in a region of multiple inversion episodes; southern South Africa. Journal of Structural Geology, 28, 1933-1947.

Perri, E. and Tucker, M., 2013. Bacterial fossils and microbial dolomite in Triassic stromatolites. Geology, 35, 207-210.

Ratner, M. and Tiemann, M., 2013. An Overview of Unconventional Oil and Natural Gas: Resources and Federal Actions. CRS Report, 27p.

Rimmer, S.M., 2004. Geochemical paleoredox indicators in Devonian-Mississippian black shales, Central Appalachian Basin (USA), Journal of Chemical Geology, 206, 373-391.

Ross, D.J.K. and Bustin, R.M., 2009. Investigating the use of sedimentary geochemical proxies for palaeoenvironment interpretation of the thermally mature organic rich strata: Examples from the Devonian and Mississippian shales, Western Canadian Sedimentary Basin. Journal of Chemical Geology, 260, 1-19.

Roswell, D.M. and De Swart, A.M.J., 1976. Diagenesis in Cape and Karroo sediments, South Africa, and its bearing on their hydrocarbon potential. Transactions of the Geology Society of South Africa, 79, 81-145.

Rubidge, B.S., Hancox, P.J. and Catuneanu, O., 2000. Sequence analysis of the Ecca-Beaufort contact in the southern Karoo of South Africa. South African Journal of Geology, 103, 81-96.

Rubidge, B.S., Hancox, P.J. and Mason, R., 2012. Waterford Formation in the south-eastern Karoo: Implications for basin development. South African Journal of Science, 108, 119-123.

Rubidge, B.S., Erwin, D.H., Ramezani, J., Bowring, S.A. and de Klerk, W.J., 2013. High-precision temporal calibration of late Permian vertebrate biostratigraphy.: U-Pb constraints from the Karoo Supergroup, South Africa. Geology, 41, 363-366.

Scheffler, K., Bühmann, D. and Schwark, L., 2006. Analysis of late Palaeozoic glacial to postglacial sedimentary succession in South Africa by geochemical proxies-Response to climate evolution and sedimentary environment. Palaeogeography, Palaeoclimatology, Palaeoecology, 240, 184-203.

Schoenherr, J., Littke, R., Urai, J.L., Kukla, P.A. and Rawahi, Z., 2007. Polyphase thermal evolution in the Infra-Cambrian Ara Group (South Oman Salt Basin) as deduced by maturity of solid reservoir bitumen. Organic Geochemistry, 38, 1293-1318.

Schoepfer, S.D., Shen, J., Wei, H., Tyson, R.V., Ingall, E. and Algeo, T.J., 2014. Total organic carbon, organic phosphorous, and biogenic barium fluxes as proxies for paleomarine productivity. Earth Science Reviews in press. doi:10.1016/earscirev.2014.08.017

Scheiber-Enslin, S.E., Webb, S.J. and Ebbing, J., 2014a. Geophysically Plumbing the Main Karoo Basin, South Africa. South African Journal of Geology, 2014, 117, 275-300 doi:10.2113/gssajg.117.2.275

Scheiber-Enslin, S.E., Ebbing, J. and Webb, S.J., 2014b. An integrated geophysical study of the Beattie Magnetic Anomaly, South Africa. Tectonophysics 636, 228-243

Small, M.J., Stern, P.C., Bomberg, E., Christopherson, S.M., Goldstein, B.D., Israel, A.L., Jackson, R.B., Krupnick, A., Mauter, M.S., Nash, J., North, D.W., Olmstead, S.M., Prakash, A., Rabe, B., Richardson, N., Tierney, S., Webler, T., Wong-Parodi, G. and Zielinska, B., 2014. Risks and Risk Governance in Unconventional Shale Gas Development. Environmental Science and Technology, 48, 8289-8297

Smith, R.M.H., 1990. A review of the stratigraphy and sedimentary environments of the Karoo Basin, South Africa. Journal of African Earth Sciences, 10, 117-137.

Smith, R., Eriksson, P. and Botha, W., 1993. A review of the stratigraphy and sedimentary environments of the Karoo-aged basins of southern Africa. Journal of African Earth Sciences (and the Middle East), 16, 143-169.

Smith, R.M.H. and Botha-Brink, J., 2014. Anatomy of mass extinction: Sedimentological and taphonomic evidence for drought-induced die-offs at the Permo-Triassic boundary in the main Karoo Basin, South Africa. Palaeogeography, Palaeoclimatology, Palaeoecology, 396, 99-118.

Stern, P.C., Webler, J. and Small, M., 2014. Understanding the Risks of Unconventional Shale Gas Development. Environmental Science and Technology, 48, 8287-8288.

Svensen, H., Jamtveit, B., Planke, S. and Chevallier, L., 2006. Structure and evolution of hydrothermal vent complexes in the Karoo Basin. Journal of the Geological Society, London, 163, 671-682.

Svensen, H., Planke, S., Chevallier, L., Malthe-Sørenssen, A., Fernando Corfu, F. and Jamtveit, B., 2007. Hydrothermal venting of greenhouse gases triggering Early Jurassic global warming. Earth and Planetary Science Letters, 256, 554-566.

Svensen, H., Bebout, G., Kronz, A., Li, L., Sverre Planke, S., Chevallier, L. and Jamtveit, B., 2008. Nitrogen geochemistry as a tracer of fluid flow in a hydrothermal vent complex in the Karoo Basin, South Africa. Geochimica et Cosmochimica Acta, 72, 4929-4947.

Svensen, H., Corfu, F., Polteau, S., Hammer, Ø., Planke, S., 2012. Rapid magma em-placement in the Karoo Large Igneous Province. Earth and Planetary Science Letters, 325-326, 1-9. http://dx.doi.org/10.1016/j.epsl.2012.01.015.

Tankard, A., Welsink, H., Aukes, P., Newton, R. and Stettler, E., 2012. Geodynamic interpretation of the Cape and the Karoo basins, South Africa. Phanerozoic Passive Margins, Cratonic Basins and Global Tectonics Maps. USA and UK: Elsevier, 869p.

Tinker, J., de Wit, M.J. and Brown, R., 2008. Mesozoic exhumation of the southern Cape, South Africa, quantified using apatite fission track thermochronology. Tectonophysics, 455, 77-93.

Toerien, D.K. (Compiler), 1991. Geological sheet 3324 (Port Elizabeth), scale 1:250 000, Geological Survey of South Africa.

Twine, T. and Jackson, M., 2012. Karoo Shale Gas Report. Unpublished Report by Econometrix (Pty) Ltd, 74p.

Van der Merwe, W.C., Flint, S.S. and Hodgson, D.M., 2010. Sequence stratigraphy of an argillaceous, deep water basin-plain succession: Vischkuil Formation (Permian), Karoo Basin, South Africa. Marine Petroleum Geology, 27, 321-333.

Veevers, J.J., 2004. Gondwanaland from 650-500 Ma assembly through 320 Ma merger in Pangea to 185-100 Ma breakup: supercontinental tectonics via stratigraphy and radiometric dating. Earth-Science Reviews, 68, 1-132.

Viljoen, J.H.A., 1994. Sedimentology of the Collingham Formation, Karoo Supergroup. South African Journal of Geology, 97, 167-183.

Visser, J.N.J., 1992. Sea-level changes in a back-arc-foreland transition: the late Carboniferous-Permian Karoo Basin of South Africa. Sedimentary Geology, 83, 115-131.

Wang, F.P. and Gale J.F.W., 2009. Screening Criteria for Shale-Gas systems. Gulf Coast Association of Geological Societies Transactions, 59, 779-793

Wang, G. and Carr, T.R., 2012. Methodology of organic-rich shale lithofacies identification and predication: A case study from Marcellus Shale in the Appalachian basin. Computer and Geosciences, 49, 151-163.

Weckmann, U., Ritter, O., Jung, A., Branch, T. and De Wit, M.J., 2007. Magnetotelluric measurements across the Beattie magnetic anomaly and the Southern Cape Conductive Belt, South Africa. Journal of Geophysical Research, 112, B5, B05416.

White, W.M., 2013. Geochemistry. John Wiley & Sons, Ltd, U.S.A., 688p.

Wickens, H. de V., 1994. Basin Floor Fan building Turbidites of the South Western Karoo Basin. Permian Ecca Group, South Africa. PhD thesis, University of Port Elizabeth, Port Elizabeth, 233p.

Zoback, M.D. and Arent, D.J., 2014. The opportunities and challenges of sustainable shale gas development. Elements, 10, 251-253.

Editorial handling: L.D. Ashwal.

Appendix-Methodology

Thin section microscopy

Thin section analysis was undertaken using a Zeiss Axiophot polarizing microscope with an attached AxioCam digital camera, which is connected via fiber-optic cable that allows for fast imager transfer. Samples were examined for rock textures, grain size, mineral identification, mineral assemblages, sedimentary structures, biogenic structures and palaeontology

Scanning-Electron Microscopy (SEM)

SEM was carried out with the Ultra 55 Plus (Carl Zeiss SMT), which has a tungsten-zircon field-emission filament, an acceleration voltage of 0.02 to 30 kV, resolution of 1.0 nm at 15 kV, probe current of 4 pA-20 pA, Inlens SE and in-column BSE detectors (EsB), ET-SE detector, angle selective BSE detector (AsB), ultraDry SDD (EDS) detector and a panchromatic (imaging) CL detector. SEM was carried out on freshly broken, Au-covered samples to observe the internal structure, intergranular porosity, micro-textures and to determine elements (i.e. identify mineral constituents).

X-Ray Diffraction (XRD)

Two grams of dried powdered sampled material is packed into metal discs and inserted in the Bruker-axs D5000. Programs used for data analysis are Eva and Autoquan. Eva can identify minerals by comparing the generated peaks to peaks from existing mineral information in a database.

X-Ray fluorescence (XRF)

XRF analyses powdered samples which were melted in Pt-Au and set into glass discs. Analyses were performed using PANalytical AXIOS Advanced containing an end-window Rhodium-X-ray tube SST-MAX with 4 kW output and LiF analyser crystal. The resulting data were interpreted using the computer program ModAn. It is assumed that the sulfur content in the samples is associated with pyrite, therefore sulfur and its associated iron is subtracted and results are recalculated to 100%. The bulk sulfur content is calculated using a carbon sulfur determinator (ELTRA CS 2000 Carbon Sulfur Determinator).

TOC/Rock Eval analysis

Total organic carbon (TOC) contents were analyzed using a LECO™ CNS-2000 elemental analyser, and Rock-Eval parameters using a Rock-Eval 6 instrument. Rock-Eval pyrolysis technique is used to identify the hydrocarbon release of organic rich sedimentary rocks, which helps to characterise the maturity and type of the organic matter within the rock. Rock Eval measures the hydrogen/carbon ratio (H/C) and the oxygen/carbon ratio (O/C). These ratios are related to the hydrogen index and the oxygen index, the HI values representing hydrogen richness and the OI values representing oxygen richness (Martin et al., 2008).

Vitrinite reflectance

Vitrinite reflectance is used as a parameter to measure thermal maturity in rocks. Vitrinite Reflectance was performed at RWTH Aachen University using a Zeiss microphotometric system which was calibrated with Zeiss yttrium-aluminium-garnet standard (R=0.906), using a 50x objective lens under immersion oil (n_e=1.518). Reflectance is measured by the amount of light reflected from the samples and is recorded as R_o. 100 particles were assessed per sample. Results are generated as vitrinite reflectance histograms. Jacob (1989) and Landis and Castaño (1995) showed that there is a positive linear correlation between vitrinite reflectance (VR_o) and bitumen reflectance (BR_o). As a result BR_o can be converted to VR_o which allows bitumen to be used in maturation studies in a sample where vitrinite is lacking (Schoenherr et. al., 2007).

Stable isotope analysis ($\delta^{15}N$, $\delta^{13}C$)

Ratios of stable carbon and nitrogen isotopes are fractionated during primary productivity of organic matter and may differentiate between terrestrial and marine organic matter in sedimentary rocks. $\delta^{13}C$ values between -23 and -34‰ indicate terrestrial plants and marine organic matter is typically between -22 and -20‰. $\delta^{15}N$ values of 4 ± 5‰ are typical of terrestrial plants and 7 ± 5 for marine plants (White, 2013). Degrees of fractionation may vary and the use of C/N ratios against $\delta^{13}C$ values will better help discriminate between organic matter sources. The N and TOC content and the $\delta^{15}N_{tot}$ and $\delta^{13}C_{org}$ isotopic composition were measured using the NC2500 Carlo Erba elemental analyzer coupled with a ConFlowIII interface on a DeltaplusXL mass spectrometer (ThermoFischer Scientific). Samples were loaded in capsules and burned with excess oxygen in the elemental analyzer. The released gases are flashed by a helium carrier-gas flow into the IRMS. The isotopic composition (δ) is determined by calculating the difference between the isotopic ratios (R) of the samples relative to an international standard (1).

$$\delta(‰)=\left[\frac{R_{sample}-R_{sample}}{R_{sample}}\right]\times 1000 \quad (1)$$

The ratio and standard for carbon is $^{13}C/^{12}C$ and VPDB (Vienna PeeDee Belemnite), and for nitrogen it is $^{15}N/^{14}N$ and air.

Open pyrolysis and thermovaporization

Open pyrolysis and thermovaporization are used to evaluate source rock potential by differentiating remnant hydrocarbons and hydrocarbons that it still may generate. Samples were prepared for open pyrolysis and thermovaporization respectively. For open system pyrolysis between 13 to 23 mg (more sample material is needed in samples with low TOC content) of powdered sample material is required. The powdered material is

inserted into a glass tube (26 mm long, 3 mm in diameter) and closed off at either end of the tube with purified quartz wool. The sample is analysed by a microscaled sealed vessel (MSSV) Pyrolysis injector system with an Agilent GC 6890A interface. The sample is then heated in a flow of helium up to 300°C during which pre-existing hydrocarbons are released. The sample is then further pyrolyzed by heating it at 50°C/min from 300°C to 600°C producing further hydrocarbons by 'cracking' of the kerogen at 600°C. The quantification of the individual compounds and the totals were conducted by external quantification with an *n*-butane standard. Hydrocarbon peaks are identified using reference chromatograms. For thermovaporization 20 to 30 mg of freshly crushed sample is placed in a glass tube, sealed with quartz powder and the opening of the tube is sealed by a hydrogen flame. The sample is heated up to 300°C, after which the tube is crushed and the hydrocarbons are moved to a cryogenic trap (liquid nitrogen). Thereafter the hydrocarbons move into a capillary column where they are separated and their retention times recorded similarly to the pyrolysis method.

Hg-intrusion porosimetry

The measurement of porosimetry by mercury intrusion describes the pore size, volume, distribution, density of the material and the specific surface area of the sample (Giesche, 2006). The samples were carefully broken to ensure that no artificial surfaces could seal the pores and 10 to 15 g of sample material was dried in an oven prior to mercury intrusion at 50°C for ~22 hours. The samples are placed in a dilatometer and placed in the WS 2000 Porosimeter. Mercury is inserted and pressure applied. The change in mercury level is recorded and porosity calculated with computer software.